Towards the Development of Organic Electrochemical Devices for Enveloped Virus Detection

A Thesis

Presented to the Faculty of the Graduate School

of Cornell University

In Partial Fulfillment of the Requirements for the Degree of

Master of Science

by

Cheyan Xu

August 2019

ABSTRACT

Viral infections induced by enveloped viruses have been a major public health concern for decades. In order to initiate timely antiviral therapy and reduce human mortality during a virus outbreak, a sensitive viral diagnostic technique that can rapidly detect and identify enveloped viruses is necessary. The supported lipid bilayer (SLB) is a well-established representative of a cell membrane that mimics the outer biological surface of a host cell. It is commonly formed on electrically inert, planar, silica-based surfaces and have been used with great effect to characterize virus-host interactions. However, these studies require the virus to be fluorescently labeled prior to study. Therefore, we proposed to form these biomimetic SLBs on PEDOT:PSS, a conductive polymer support, that the charged viral genome can interact with upon fusion, resulting in an electrical readout. Challenges lie in constructing SLBs on PEDOT:PSS due to both electrostatic repulsion between the polymer and charged species in the cell membrane and the swollen polymers unfavorable surface smoothness that can prevent membrane vesicles from fusing into a planar geometry. Various stimuli were explored to successfully induce bilayer formation on the polymer surface, which includes divalent cations, charged liposomes, pegylated cushions, and external macromolecules. Furthermore, because this polymer is transparent, we could still carry out single virion fusion using fluorescence microscopy to corroborate the ability to successfully test the electrical sensing in the future. This critical work demonstrates the potential for this platform to become a new kinds of viral detection device.

BIOGRAPHICAL SKETCH

Cheyan Xu grew up in Dalian, China. In 2017, Cheyan received his B.S.E in Chemical Engineering from Case Western Reserve University. He pursued a M.S degree in the Department of Chemical and Biomolecular Engineering at Cornell University in Susan Daniel's group. He investigated the use of an organic electrochemical transistor that can detect and identify enveloped viruses. Particularly, he developed a new technique to form supported lipid bilayers on a conductive polymer, PEDOT:PSS, incorporated viral receptors into the bilayers via cell blebbing and characterized viral fusion kinetics of Influenza X-31 viruses. In his work, he integrated several technologies and techniques including cell culture, fluorescence microscopy, microfluidic device and QCM-D.

I would like to dedicate this thesis to my family and friends who continued to support me throughout this process. Without their help, none of this would have been possible.

ACKNOWLEDGMENTS

The research presented in this thesis would not have been possible without the generous help and support from members of the Cornell community, especially those in the department of Chemical and Biomolecular Engineering. I would like to thank my advisor, Prof. Susan Daniel and my special committee member, Prof. Christopher K. Ober for their guidance and instructions. I thank all the members of the Daniel Research Group for their coaching and collaborations. I would also like to thank Dr. Anna-Maria Pappa for training me on using electrochemical device. Finally, I would like to thank my family and my girlfriend for their encouragement and support throughout my study abroad period. All of this would not be possible without them. Grants and funding are acknowledged at the end of each chapter.

TABLE OF CONTENTS

LIST OF FIGURES

LIST OF TABLES

LIST OF ABBREVIATIONS

DTT – dithiothreitol

FRAP – fluorescence recovery after photobleaching

GOPS – (3– glycidyloxypropyl)trimethoxysilane

GPI-YFP – glycophosphatidylinositol anchored yellow fluorescent protein

GPMV – giant plasma membrane vesicle

HEK – human embryonic kidney

OECT – organic electrochemical transistor

P2X2-neon – P2X2 receptor fused to a neon green fluorescent protein

PDMS – polydimethylsiloxane

PD-SLBs – supported lipid bilayers formed on PEDOT:PSS

PEDOT:PSS – Poly(3,4-ethylenedioxythiophene) doped with poly(styrene sulfonate)

PEG – polyethylene glycol

QCM-D – quartz crystal microbalance with dissipation

R18 – Octadecyl Rhodamine B chloride

RT-qPCR – reverse transcription polymerase chain reaction

SLB – supported lipid bilayer

SPT – single particle tracking

TGE – total ganglioside extract

TIRFM – total internal fluorescence microscopy

PREFACE

Background Information

Viral infections induced by human pathogenic enveloped viruses have become a major cause of human death and disease. Although prophylactic and therapeutic treatments have been developed for certain types of the viruses, such as influenza and hepatitis B virus[1-4], a potent medication is still lacking for the majority of the infective agents. Furthermore, for viruses that have been successfully treated before, a timely therapy may not be initiated due to a lack of techniques that are sensitive enough to rapidly diagnose various subtypes and strains within the same virus species. For example, during the 2017-2018 season, a total number of 959,000 hospitalizations and 79,400 deaths from influenza A and B viruses were estimated in the United States[5]. Vaccines are produced each year to protect the populations, but influenza, like other viruses, continuously evolves. This continuous viral evolution requires scientists to constantly improve the existing diagnostic techniques to sensitively detect those emerging strains and correctly diagnose people in the initial stage of a virus infection.

During the past decades, numerous viral detection methods have been established in order to control the health burdens generated by enveloped viruses[6-10]. These methods utilize different techniques, including antibody avidity, cell culture, immunofluorescence assay as well as PCR, and have all been successfully used to detect and identify viruses. Among these established approaches, reverse transcription PCR (RT-qPCR) is one of the most sensitive and reliable tools to analyze viruses in the early stage of an infection. This is because of its distinct ability to amplify the small amount of viral genetic materials that would be available for analysis during that

period[11]. However, though powerful, the risk of contamination and the complexity in daily operation make RT-qPCR relatively difficult to popularize, especially in underdeveloped areas[12]. Moreover, detections based on more straightforward techniques also have their own drawbacks. For instance, some diagnosis can be made by measuring antibodies produced in the host in response to viruses[9,13]. These tests are simple, cheap, fast and specific, but diagnosing enveloped viruses using such methods are challenging[14]. Due to sub-optimal test sensitivity of the techniques, antibodies cannot be detected until a significant immune response has been initiated. This delays the viral diagnosis process, which further increases the difficulty in the early detection of enveloped viruses.

As obligatory intracellular parasites, enveloped viruses must transfer their genetic materials across the host cell membranes, by which they can further infect their hosts and propagate progeny virions (Fig. 1)[15]. Their outer lipid membranes, therefore, must merge with the host cell membranes and form individual fusion pores to allow the genomes to escape. By leveraging the natural propensity of enveloped viruses to fuse into their host lipid bilayers, multiple viral quantification platforms have been developed so that researchers could assess virus-host interactions effectively and safely[18-20]. One crucial element in these devices is a supported lipid bilayer (SLB) that forms in microfluidic channels and behaves as a host cell membrane mimic.

A supported lipid bilayer is one of the most representative model membranes that can mimic the outer biological surface of a cell. It maintains both the natural components within the bilayer and its lipid fluidity[21,22]. These are two crucial

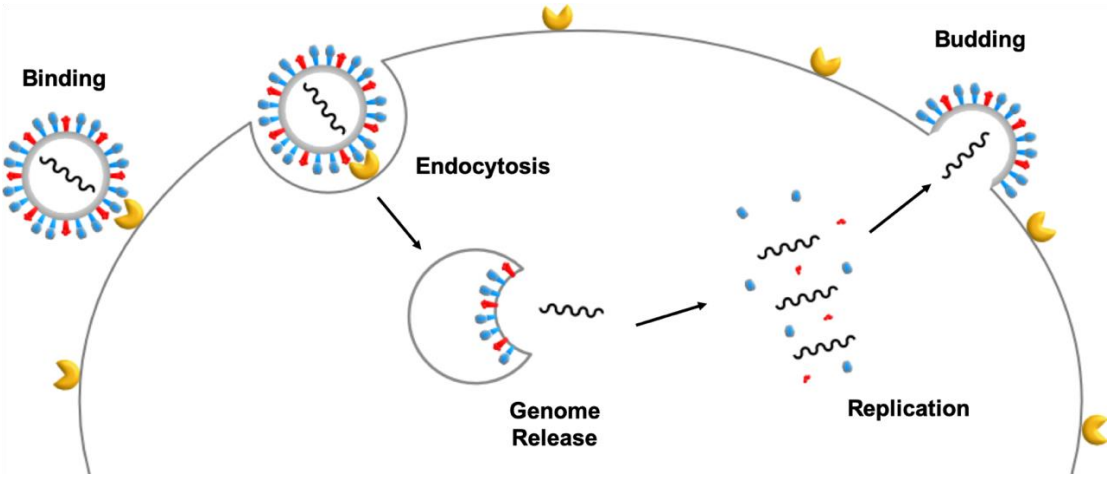

Fig. 1 **The *in vivo* process of class I viral entry.** The fusion protein (blue) of the viral particle binds to its specific receptor (yellow) on the host cell membrane (light grey). The protein then goes through a conformational change, which brings the particle into an endosome. As the pH around the endosome goes down, a viral fusion event is triggered, and genomes are released into the host cell. After the released genomes being replicated within the cell, new viral particles will bud at the surface of the host cell membrane and attack other cells.

requirements in order to study virus-cell interactions as well as membrane fusion. The maintenance of natural components within an SLB ensures the availability of viral receptors that are specific for viruses to bind to. Meanwhile, the mobility of the bilayer allows the merging of viral envelops into the model membrane through diffusion. In addition, the planar geometry of an SLB simplifies the innate complexity of a cell by isolating the outer lipid membrane from encapsulated cytosolic components, enabling studies of cellular activities that interact with the biological interface specifically. This further allows quantifications of viral fusion kinetics using fluorescence microscopy because of the compatibility of an SLB with a cover slide[21,23]. However, because the glass substrate is inert, it can perform merely as a solid support for the biomimetic platform without any additional functionalities. This reduces the efficiency of spatial utilization and the potency of the characterization tool. Therefore, a novel idea was proposed by our group to extend the application of an SLB from a passive

characterization platform to an electrochemical viral diagnostic device that can actively detect and identify enveloped viruses using electrical means.

As mentioned above, RT-qPCR is one of the most popular virus identification techniques because of its ability to drastically increase the viral genome concentration, which enables early determinations of the pathogens. Similarly, one of the most important advantages of diagnosing viruses using electrical measurements is their capability to detect a small amount of virus genomes by means of organic electrochemical transistors (OECTs)[22]. Nevertheless, instead of quantitatively enhancing the concentration of genetic materials, an organic electrochemical transistor leverages its high sensitivity[25] to capture small electrical signal changes occurring in the system, which are triggered by the release of charged virus genomes. Afterwards, the weak signals recorded by the devices can be amplified for future characterizations and, ultimately, provide an innovative solution to the difficulty in viral diagnosis during the initial stage of an infection.

In our OECT concept (Fig. 2), an SLB that carries numerous receptors of influenza viruses is assembled on the channel material, poly(3,4-ehylenedioxythoiphene) doped with polystyrene sulfonate (PEDOT:PSS), inside of the transistor. Like various enveloped viruses, flu particles have the propensity to bind to their receptors, fuse into the host membrane after acidification and release their genomes[24]. Because viral genomes are charged molecular complexes, they can potentially change the conductivity of the polymeric channel upon release and interaction with the conducting polymer. Thus, by adding viruses into the electrolyte

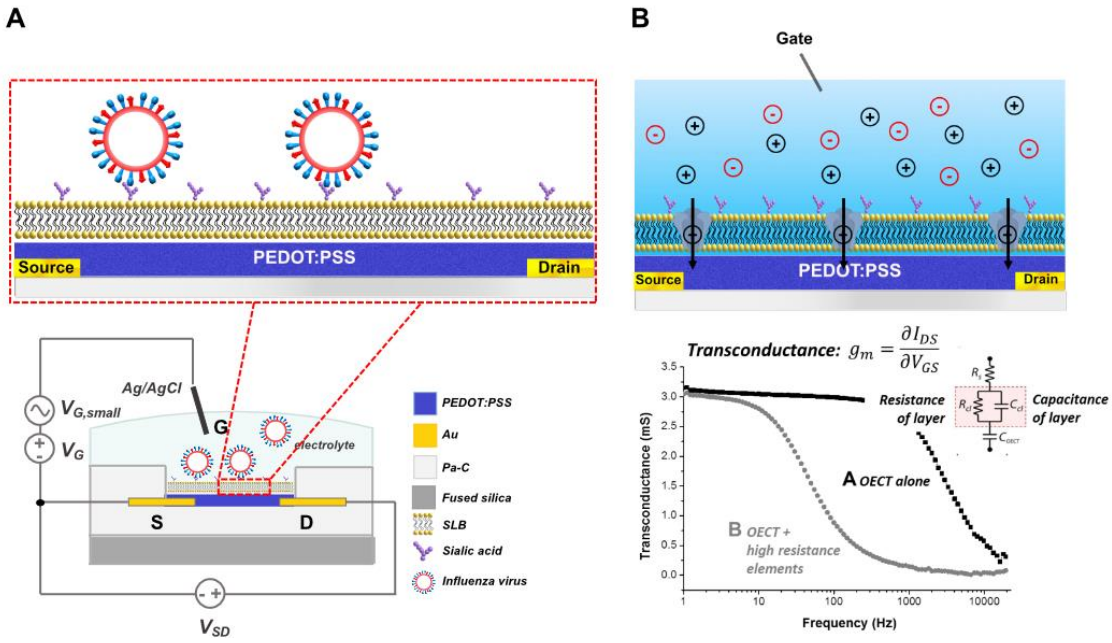

Fig. 2 **Illustration of the bio-sensor concept. (A)** The organic electrochemical transistor contains a conductive polymer channel, PEDOT:PSS, which is in direct contact with the electrolyte solution. By forming a supported lipid bilayer (SLB), a representative model membrane, on the channel, researchers will be able to detect and identify the enveloped viruses that bind to their specific receptors on the SLB based on the impedance change of the bilayer. **(B)** The device consists of source (S), drain (D) and gate (G) electrodes. Once the gate electrode applies a potential into the solution, ions will then enter the PEDOT:PSS channel and change its conductivity. Because a common SLB is resistive, it will impede the ions flux to some extent based on the availability of ion channels (*top*). A sample illustration of the changes in the transconductance of the device before and after forming a lipid bilayer (*bottom*).

solution, we hypothesize that we will be able to detect and identify them by observing the change of electrical signals induced by genome release.

However, building such devices using OECT requires a lot of optimization, as a transistor contains multiple layers of materials whose interactions with membrane components within an SLB remain unknown. Hence, an electrode arrangement was studied first using the channel material, PEDOT:PSS, as a simpler version of the electrochemical device to optimize experimental conditions for the future development of the transistor. In addition, because of the high transparency of the polymer film[23], common bilayer characterization techniques such as FRAP (fluorescence recovery

after photobleaching) and TIRFM (total internal reflection fluorescence microscopy) were performed to 1) optimize SLB formations on the PEDOT:PSS electrode and 2) determine the compatibility of the device with viral fusion analysis[18,19,21]. As supported lipid bilayers play a fundamental role for the entire project, in the first chapter of this thesis, various strategies and characterizations are introduced in order to form continuous supported lipid bilayers on PEDOT:PSS.

CHAPTER 1

Supported Lipid Bilayer Assembly on PEDOT:PSS Channel in an Organic Electrochemical Device

1.1. Introduction

Membrane proteins perform several important biological roles in cellular activities, such as transport channels, surface receptors, enzymes, cytoskeleton and recognition markers[25]. Important to this work is their role as receptors for virus targets. However, due to their complicated structures and dynamic lipid surroundings, studying the functions of membrane proteins becomes a challenging task. In order to understand the mechanisms of protein functions and how these activities are regulated by the lipid environment, model bilayer systems become common characterization platforms because they retain critical membrane components and two-dimensional lipid fluidity[28,29]. Among many established model membranes, the supported lipid bilayer (SLB) is one of the most representative ones due to its distinct planar geometry which makes it compatible with many surface characterization techniques, such as FRAP, TIRFM[18,19,21,23], and quartz crystal microbalance with dissipation (QCM-D)[28]. While being utilized under various circumstances, SLBs have not been fully exploited yet because of their inert substrate (See *Background Information*).

Pioneered by McConnell et al. in 1985[29], SLBs have been assembled mainly on hydrophilic silica-based surfaces. Liposomes used to form[30] or induce[22] the formation of SLBs are amphiphilic with their hydrophilic headgroups facing outwards (Fig. 3A). When the surface of a liposome touches the hydrophilic substrate (e.g.

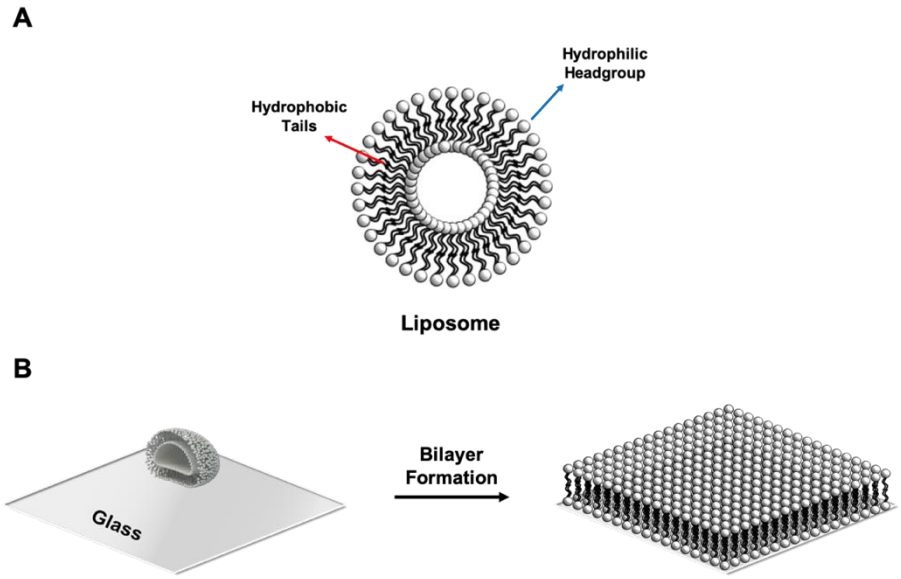

Fig. 3 **Illustration of a lipid vesicle and the bilayer formation process (A)** A typical liposome used to form a supported lipid bilayer contains an aqueous core (e.g. PBS buffer) surrounded by an amphiphilic phospholipid bilayer. An amphiphilic phospholipid consists of a hydrophilic headgroup and two hydrophobic tails. In aqueous environment, lipid molecules aggregate together and form a spherical shape with the hydrophilic headgroups facing outwards to protect their hydrophobic tails from outer solution. **(B)** A microscope cover slide is treated with piranha solution to make its surface clean and hydrophilic. Liposomes are then deposited onto the surface and deformations are caused due to Van der Waals interactions between the vesicles and underneath piranha-treated surface. Once the deformation of a vesicle reaches a threshold, it will rupture and form a planar patch on the glass slide. This will induce the rupture of adjacent vesicles because their hydrophilic surfaces are in direct contact with the hydrophobic tails of the planar patch.

piranha-treated glass), the spherical vesicles will deform, rupture and eventually pave a planar bilayer on the surface if the Van der Waals force is strong enough (Fig. 3B). Based on this, a strategy was developed by our group to incorporate natural membrane components into SLBs on glass using synthetic lipids and cell blebs[21,33]. Cell blebs are a type of proteoliposome that buds off from cell membranes, which can be induced by chemical means[32]. Because they are derived directly from the plasma membranes, these membrane vesicles maintain the same components as those naturally available in the biological membranes, importantly here, the virus receptor. A simple illustration of our strategy to rupture blebs on glass is shown in Fig. 4. Basically, blebs are first

absorbed onto a glass substrate, but they cannot rupture spontaneously because proteins and cholesterol inside of their membranes increase the mechanical strength of the vesicles. To construct a bleb bilayer on glass, synthetic lipids are introduced as fusogenic vesicles because they spontaneously rupture on a hydrophilic surface, which then induces the rupture of neighboring cell blebs. Platforms built with the same strategy have been applied to various fields such as viral fusion analysis[19,21] and antibacterial drug development[33]. Nevertheless, though silica-based surfaces demonstrate a great potential as carriers for biomimetic platforms, these materials are electrically insulating and can denature proteins if they contact them, which significantly limits the applications of the platforms.

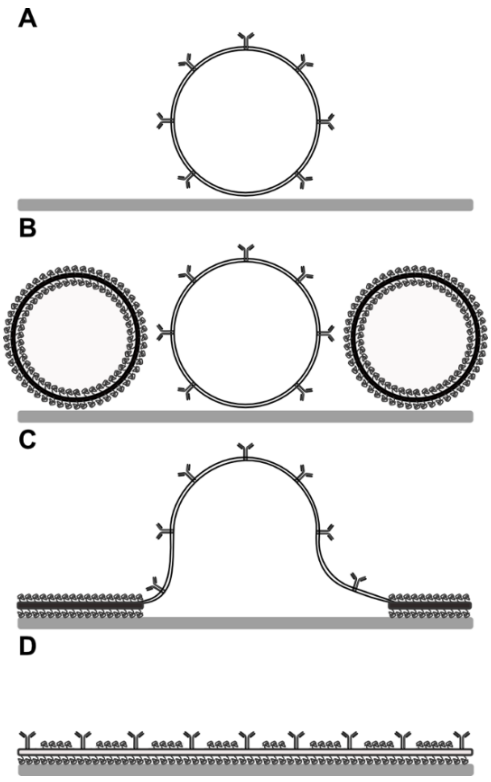

Fig. 4 **Illustration of PEGylated bleb bilayer formation on glass slides.** Cell blebs or membrane vesicles (white circle) are deposited onto the glass substrate and PEGylated fusogenic vesicles (black lipid circle with brown polymer cushion) are added. Fusogenic vesicles rupture spontaneously on hydrophilic surface which induces the rupturing of adjacent blebs. A "parachuting" rupture mode was determined from an enzymatic analysis.

During the past decade, organic electrochemical transistors (OECTs) have demonstrated a great potential in interfacing with biology[23]. One major advantage of OECTs is their efficient transduction of ionic fluxes, which are common in biological applications, into electrical signals. Within the group of OECTs, poly(3,4-ethylenedioxythoiphene) doped with polystyrene sulfonate (PEDOT:PSS) is one of

the most highly attractive channel materials. Its attractiveness stems for its high conductivity, low production cost, good optical transparency, and great stability[25,36]. In addition, as a result of its relatively soft polymeric surface which resembles in form the cytoskeleton that naturally surrounds the cell membrane[35], PEDOT:PSS provides a promising solution to the protein denaturation resulting from the direct contact with solid surfaces such as mica and glass. This, in combination with its transduction functionality, makes PEDOT:PSS an exceptional target for the viral detection application as discussed before.

Unfortunately, constructing an SLB platform that closely mimics the host cell membrane on PEDOT:PSS is a challenging task for multiple reasons. First, PEDOT:PSS is negatively charged with its zeta potential reported as around -75 mV[36]. While not necessarily the same as the polymer, charges carried by most liposomes (e.g. POPC, DOPC, POPS, etc.) that are involved in bilayer formation are neutral to negative. Multiple studies have revealed that the electrostatic interactions between support and lipids could influence the adsorption of lipid vesicles[37] and simultaneously reduce the deformation of adsorbed liposomes caused by hydrophilic-hydrophilic interactions. This obviously makes PEDOT:PSS an unfavorable surface for vesicle rupture as well as bilayer formation. Second, though resembling cytoskeleton surroundings, the polymeric surface of PEDOT:PSS would not contribute to vesicle fusion because liposomes tend to fuse on smooth, clean, and hydrophilic films[26]. This condition is hard to meet because PEDOT:PSS swells under aqueous solution[38]. Therefore, in order to build a viral diagnostic platform based on supported lipid

bilayers and PEDOT:PSS channel, additional treatments must be implemented to offset the electrostatic interactions and reduce the energy barrier for vesicle fusion.

In this chapter, we investigated the implementation of different strategies in order to assemble SLBs on PEDOT:PSS using synthetic lipids and/or cell blebs. In particular, the spin coating speed while preparing PEDOT:PSS layers was first optimized by comparing the bilayer quality under various conditions using fluorescence microscopy. During this process, positively charged lipids, DOTAP (Fig. 5), were mixed with common fusogenic vesicles, DOPC, to reduce the electrostatic repulsion from substrates to liposomes. At the same time, an osmotic pressure difference was generated across liposome membranes by adding a polymer solution into the bulk environment. This osmotic pressure enabled water molecules within liposomes to pass through the hydrophobic tails (See Fig. 3 A as a reference for liposome structure), which enhanced the possibility of liposome membrane disruption due to thermodynamic instability. Together, these two strategies worked effectively to rupture membrane vesicles and successfully form continuous SLBs on PEDOT:PSS (PD-SLBs). However, both DOTAP and DOPC were later substituted by divalent cations and POPC respectively. This was necessary because DOTAP and DOPC are

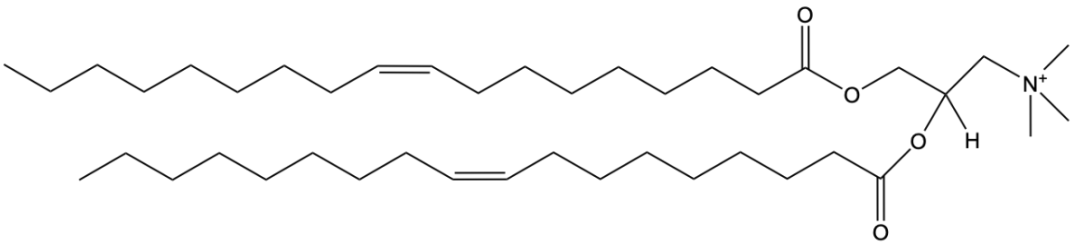

Fig. 5 **Molecular structure of DOTAP.** While many lipids such as POPC and DOPC are zwitterionic, DOTAP has only positive charge in it, which results in its high affinity to negatively charged surface as well as other membrane compounds with opposite charges.

not naturally available in cell plasma membranes and liposomes mixed with DOTAP have the propensity to aggregate on the surface after forming a continuous SLB. Eventually, by preparing fusogenic vesicles with the latter, more physiological approach, SLBs with decent diffusivity, high percentage of mobility, and adequate incorporation of viral receptors (Chapter 2) were successfully formed on PEDOT:PSS.

1.2. Materials and methods

1.2.1. Cell lines

Vero E6 and HEK (Human Embryonic Kidney) cells used in experiments were obtained from the American Type Culture Collection and grown in Dulbecco's modified Eagle's medium (DMEM; CellGro) supplemented with 10% heat inactivated fetal bovine serum (Gibco), penicillin streptomycin solution (5000 I.U./mL Penicillin and 5000 μg/mL streptomycin; CellGro) and 1% HEPES buffer (CellGro) in a 37 °C, 5% CO_2 incubator (ESCO).

1.2.2. Liposome preparation

1-Oleoyl-2-palmitoyl-sn-glycero-3-phosphocholine (POPC), 0.5% (mol/mol) 1,2-dipalmitoyl-sn-glycero-3-phosphoethanolamine-N-[methoxy(polyethylene glycol)-5000] (PEG5000-PE), 1,2-dioleoyl-sn-glycero-3-phosphocholine (DOPC), and 1,2-dioleoyl-3-trimethylammonium-propane (DOTAP) were purchased from Avanti Polar Lipids. The liposomes were prepared in glass vials by mixing a certain amount of lipids in chloroform (Sigma) to achieve the desired composition ratio. The vials were placed under a stream of nitrogen for 5 minutes and then desiccated for 3 hours to evaporate any chloroform. Phosphate buffered saline (PBS) buffer (5 mM

NaH_2PO_4, 5 mM Na_2HPO_4, 150 mM NaCl at pH 7.4) was then added to mix with the dried lipid films so that the concentration of liposomes became 2 mg/mL. The lipid mixture was then frozen overnight at -20 °C, thawed next day and extruded using a 50 nm membrane for at least 15 times. Four lipid compositions were used in this work, which are pure POPC, 99.5% POPC with 0.5% PEG5k (mol/mol), pure DOPC and 80% DOPC with 20% DOTAP (mol/mol). After preparation, liposomes were stored under 4 °C for at most one week until use.

1.2.3. Membrane bleb preparation

10 mL of 5.0×10^5 cells/mL were seeded in a 10 cm Petri dish (Corning) and incubated in a 37 °C, 5% CO_2 incubator for 24 hr. If necessary, transfections were performed by adding 15 μL of Turbofect (Thermoscientific) and10 μg of DNA plasmid in the dish, followed by another 24-hour incubation under the same condition. After this, cells were rinse with GPMV buffer (2 mM $CaCl_2$, 10 mM HEPES, 150 mM NaCl at pH 7.4) and subsequent blebbing was performed by adding 4 mL of blebbing buffer which consists of 2 mM dithiothreitol (Sigma) and 25 mM formaldehyde (Sigma) in GPMV buffer. The cells were incubated for 2 hr at 37 °C and the media was then transferred to a 15 mL ultracentrifuge tube. The tube was placed on ice for 15 min, after which the top supernatant was carefully pipetted and transferred to a new tube.

1.2.4. PEDOT:PSS slide preparation (Fig. 6)

Glass slides (25 × 25 mm No. 1.5, VWR) were cleaned with piranha solution (30% (v/v) H_2O_2 (Sigma 50 wt%) and 70% (v/v) H_2SO_4 (BDH)) for 10 min and then

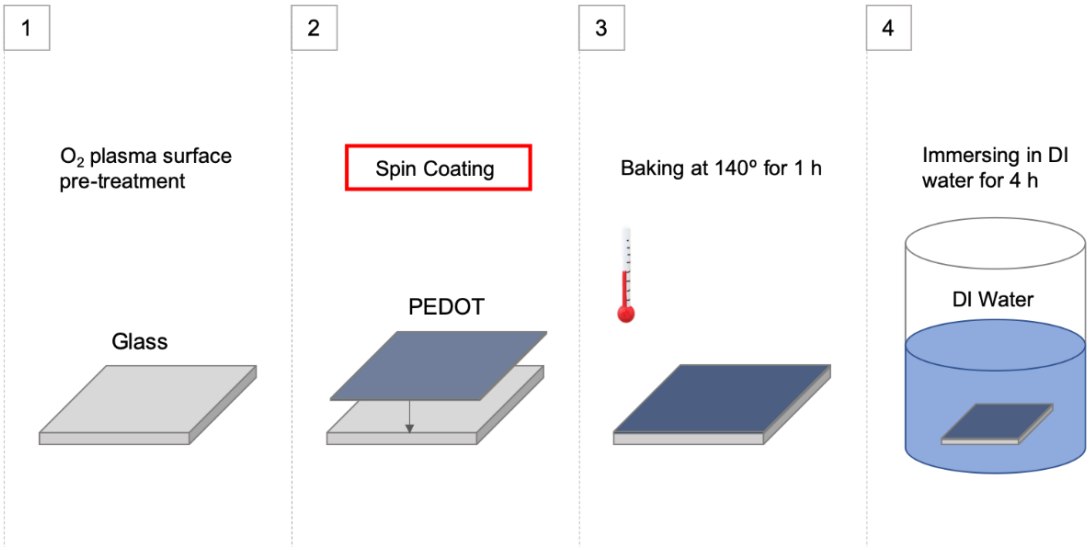

Fig. 6 **Preparation of glass slides coated with PEDOT:PSS.** PEDOT:PSS was spun on SiO_2 substrates, followed by annealing for 1 hour at 140 °C. Afterwards, the slides were immersed under DI water for 4 hours, dried with nitrogen gas and stored under the room temperature for no longer than 3 days. Different spin speeds were set while coating PEDOT:PSS dispersion onto glass substrates so that films with different thickness were coated on the surface.

rinsed for 30 min under 18.2 MΩ-cm water (ELGA Purelab Ultra, Woodridge, IL). Slides were kept immersing under 18.2 MΩ-cm water for no long than 3 days until use. PEDOT:PSS dispersion was prepared by mixing 5% (v/v) ethylene glycol (Sigma-Aldrich), 0.002% (v/v) DBSA (Sigma-Aldrich) and 1% (w/w) GOPS (Sigma-Aldrich) with Clevios PH 1000 (Heraeus Clevios GmbH). The dispersion was sonicated in a sonication bath for 30 min to reduce aggregations before use. Glass slides were then dried with nitrogen, O_2 plasma cleaned at 150 W for 2 min and coated with the PEDOT:PSS dispersion by spin-coating at 4000 rpm for 30 s. After a homogeneous film covered the entire surface, substrates were baked at 140 °C for 1 h, followed by 4 h immersion under 18.2 MΩ-cm water. Polydimethylsiloxane (PDMS) was made by 10:1 elastomer/crosslinker mixture of Sylgard 184 (Robert McKeown

Company) and baked for 3 h at 65 °C to cure to a solid phase. Then, a 5 mm diameter, 3 mm thick hole was drilled in each piece to make a PDMS well.

1.2.5. Characterization of bleb size and concentration

Nanosight NS300 (Malvern) was used to determine the size distribution and concentration of cell blebs in the GPMV solution. Before characterization, samples were diluted 1 to 100 using PBS buffer.

1.2.6. Formation of supported lipid bilayers on PEDOT:PSS for fluorescence microscopy

Preparation: Before use, PEDOT:PSS slides were activated by O_2 plasma at 25 W for 2 min and PDMS wells were affixed onto the dry, clean slides. In order to observe SLBs under fluorescence microscopes, a membrane-intercalating fluorophore, Octadecyl rhodamine (R18, Molecular Probles), was doped into membrane vesicles (e.g. cell blebs for supported bleb bilayer, or liposomes for supported lipid bilayer). Unincorporated probe was removed using a G25 spin column (GE Healthcare, Buckinghamshire, U.K.).

Three-step method for bleb bilayer: 70 µL of blebs solution at approximately 4 × 10^8 blebs/mL was first incubated in the well for 15 min (step 1). Then, 70 µL of fusogenic liposomes were added at 1 mg/mL and incubated for additional 15 min (step 2). Afterwards, bleb bilayer formation was induced by adding 100 µL of soluble polyethylene glycol 8000 (60% w/v PEG-8000, VWR) into the solution and incubated for 60 min (step 3). The well was rinsed gently with PBS buffer between each step and rigorously after the formation of a bleb bilayer to remove any unabsorbed materials (Fig. 7).

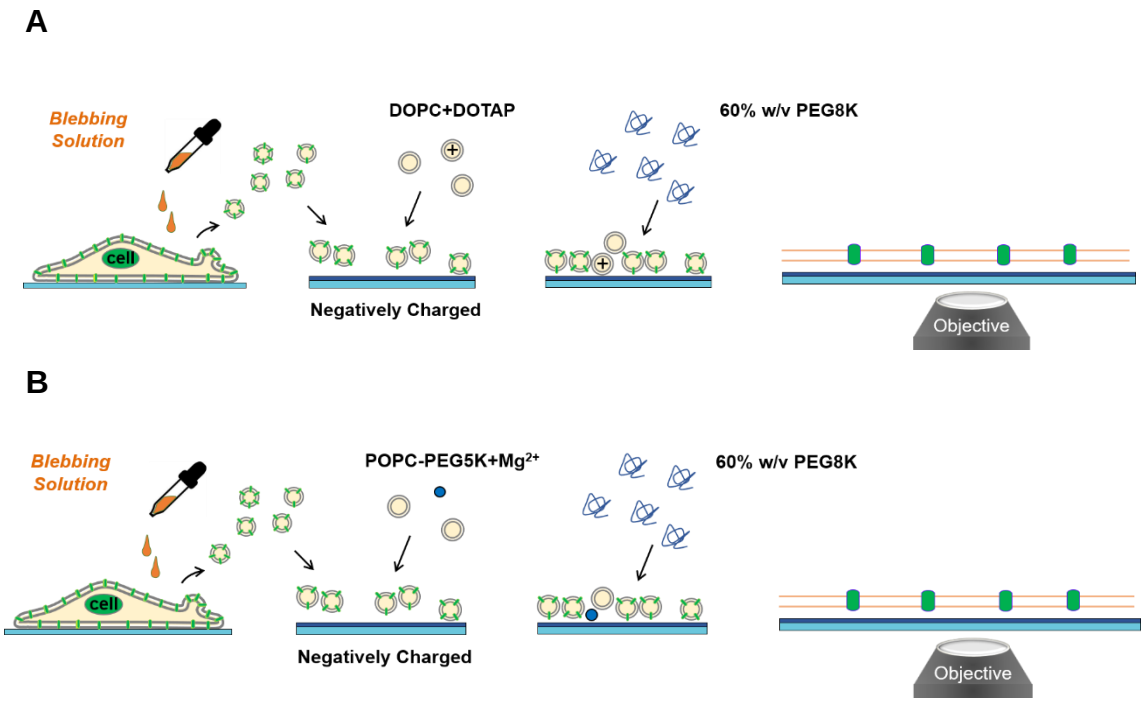

Fig. 7 **Illustration of two strategies of forming supported bleb bilayers on PEDOT:PSS substrates.** Host cells with specific receptors (green lines) for an enveloped virus are induced to generate cell plasma membrane blebs, which are subsequently absorbed on the PEDOT:PSS surface (dark blue). Then, fusogenic vesicles are deposited onto the surface with the help of **(A)** cationic liposomes, DOTAP, or **(B)** divalent cations using electrostatic force. Finally, PEG solution is added into the system, which generates a strong osmotic shock and ruptures the cell blebs to form a planar supported lipid bilayer.

Two-step method for pure lipid bilayers: Similar procedures were followed to form pure lipid bilayers on PEDOT:PSS, but instead of adding fusogenic liposomes, it is the liposomes themselves that were used as the main material for the SLB. In other words, the bleb adsorption step was skipped.

1.2.7. Fluorescence recovery after photobleaching (FRAP)

An inverted Zeiss Axio Observer Z1 microscope (Zeiss) was used to carry out FRAP measurements to determine the 2D fluidity of SLBs that formed. After the formation of an SLB on PEDOT:PSS substrate, the bilayer was scratched gently with a dissection tool to facilitate focusing under the fluorescence microscope at the appropriate z-position of the bilayer. Afterward scratching, the bilayer was rinsed with

PBS buffer for 30 s to remove materials that were scratched off. A circular spot was bleached in the bilayer membrane by a focused light beam. If the bilayer was formed and the species within it aremobile, the fluorescence intensity will recover over time. To assess the mobility, the intensity change at the bleached spot was recorded and the diffusivity of the bilayer was calculated by fitting the recovery data to a Bessel function following a Soumpasis method[39]. The diffusivity (D) was then calculated using the equation:

$$D = \frac{w^2}{4t_{1/2}} \quad (1)$$

where w is the radius of the bleached spot and $t_{1/2}$ is the half-time of the fluorescence intensity recovery.

1.3. Results and discussion

1.3.1. Comparison of different PEDOT:PSS film thickness on bilayer formation

The selection of surfaces that can perform as supports for SLBs is somewhat limited, as liposomes have the propensity to rupture on hydrophilic, clean and smooth surfaces[26]. The PEDOT:PSS dispersion for this study contained crosslinking agents such as 3-glycidoxypropyltrimethoxysilane (GOPS) whose function was to prevent the delamination of PEDOT:PSS films and enhance the overall stability of coating layers[40]. Though stability is critical, especially for biomimetic applications, an increasing GOPS concentration results in a more hydrophobic surfaces due to the hydrophobic nature of the crosslinkers. Immersing PEDOT:PSS slides under deionized water was another key step (Fig. 5 step 4), as it removed excessive PSS

along with other small molecular components that can leach out and impact bilayer formation[41]. However, researchers have found that after being exposed to aqueous environment, PEDOT:PSS films became less hydrophilic[41].

Since a decrease in hydrophilicity was seemingly inevitable, the surface smoothness of PEDOT:PSS became a promising factor to improve the compatibility of the substrates with SLBs. For this particular study, the consequence of film morphology for the performance of vesicle fusion have been studied using HEK cell blebs as a representative illustration. The surface topology of the PEDOT:PSS film was reported to be impacted by its film thickness, which can be adjusted by changing the spin coating speed during substrate preparation (See Fig. 6 in method section as a reference)[34]. In addition, a three-step approach was used to promote bilayer formation, which includes a bleb immobilization step, a fusogenic vesicle addition step and a PEG-triggered fusion step (For a detailed description, see method). Our use of soluble PEG solution (a.k.a external PEG) after the addition of rupture vesicles has two major effects on them. First, external PEG generates a strong osmotic shock across the membrane which facilitates vesicle rupture[42]. Second, the existence of macromolecules similar to PEG creates a crowded environment around vesicles[43], which forces vesicles to fuse together. The second hypothesis was supported by the fact that smaller osmolytes such as sucrose did not induce rupture on PEDOT:PSS (data not shown here). Similar ideas were previously proposed to promote vesicle fusion on different sublayers that are much less favorable for vesicle fusion compared with glass[44,46]. The fusogenic vesicles to induce the rupture of cell blebs consisted of

80% (mol/mol) DOPC and 20% (mol/mol) positive lipid DOTAP to offset negative charges.

Different spin speeds were selected while functionalizing the glass substrates with PEDOT:PSS dispersion which resulted in different layer thickness. It is reported that spin speeds ranging from 1000 rpm to 7000 rpm will lead to different film thickness from 130 nm down to 25 nm[34]. Three spin speeds that were used in this study were 1500 RPM, 2500 RPM, and 4000 RPM. Afterwards, HEK bleb bilayers were formed on substrates with different layer thickness following the same three-step method as discussed above. Fluorescence recovery after photobleaching (FRAP) was used to confirm the formation of continuous SLBs and to obtain the two-dimensional diffusivity of the bilayers. As shown in Fig. 8, sample A contained only intact HEK blebs with no fusogenic vesicles and the photobleached spot did not recover after five minutes. This was because cell blebs did not rupture spontaneously, and fluorophores inside of the vesicle membranes could not diffuse across unruptured vesicles. Sample B, C, and D were HEK-SLBs formed on PEDOT:PSS coatings prepared with 1500 rpm, 2500 rpm and 4000 rpm respectively. Fluorescence intensity recovery at the bleached spots was observed for all three conditions, which indicates that SLBs can be formed independent of spin speeds. Recovery can only occur if the fluorophores within the vesicle membranes have fused together, ruptured, and formed a mobile planar bilayer, where fluorophores outside the bleach spot are then free to diffuse into the bleached spots and recover its intensity. However, SLBs formed on PEDOT:PSS films coated using 1500 rpm and 2500 rpm have lower average diffusivities (0.22 ± 0.20 and 0.25 ± 0.18 $\mu m^2/s$ respectively) compared with that recorded on 4000 rpm

layers ($0.50 \pm 0.16 \mu m^2/s$). Lower fluorophore diffusivities imply a lower possibility of one fluorophore molecule to diffuse to the bleached spot, which indicates less lipid vesicles were ruptured on the substrate. This corresponds to the visual observation of sample B,C and D, in which bilayers formed on 4000 rpm slides have the brightest background. In addition, the diffusivity of SLBs formed on glass slides were included as a reference, which is around $0.55 \pm 0.14\ \mu m^2/s$. This is within the same order of magnitude as bilayers formed on 4000 rpm slides. Therefore, 4000 rpm was determined to be the optimal spin coating speed among three conditions, whose

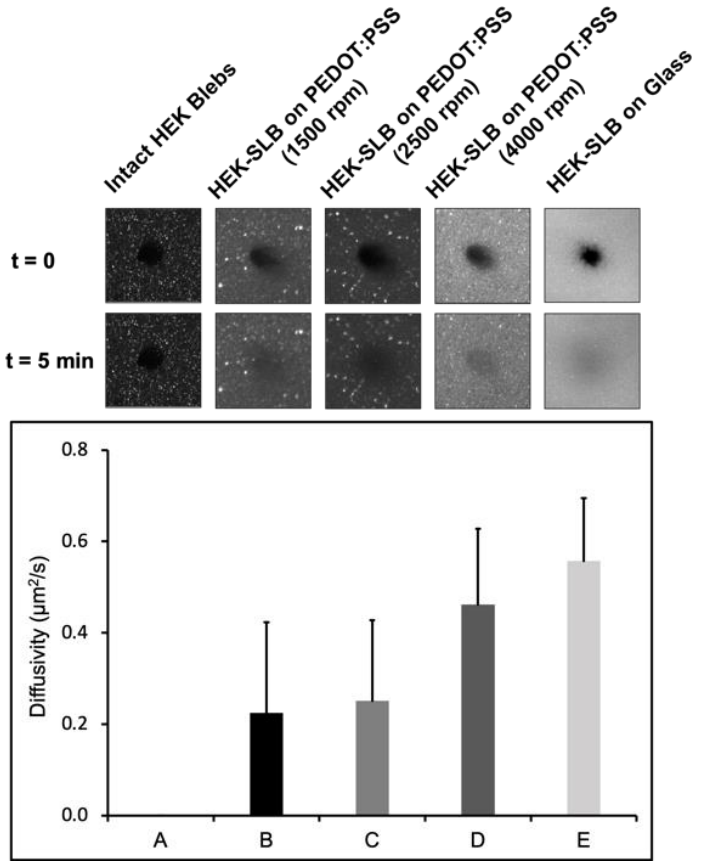

Fig. 8 **Optimization of PEDOT:PSS substrate preparation.** The fluidity of the SLBs on PEDOT:PSS coated with different spin speeds was quantified using FRAP technique and the result corresponded to that on glass slides. Note that due to the immobility of sample A, its diffusivity could not be determined.

surface smoothness is favorable to form SLBs with physiologically meaningful diffusivities. This value was then used as the standard while preparing PEDOT:PSS substrates in the following characterizations.

1.3.2. Optimization of fusogenic vesicle fusion induced by divalent cations and pegylated lipids on PEDOT:PSS

Though being implemented to successfully trigger the formation of bleb bilayers on PEDOT:PSS, DOTAP is not naturally available in virus host cell membranes and positive charges introduced by the lipid on the surface of PD-SLBs can interfere the fusion of enveloped viruses to the biomimetic platform (section 2.3.2.). Thus, a different composition of fusogenic vesicles needs to be developed to induce the rupture of cell blebs on the polymer film. An alternative to positively charged lipids that can improve the conditions for vesicle fusion and SLB formation on PEDOT:PSS is to include divalent cations in buffers while preparing PD-SLBs. Divalent cations have been shown in literature to promote bilayer formation by affecting the vesicle-substrate interaction and increasing the deformation of adsorbed vesicles[47,48]. This further reduces the threshold coverage required for liposomes to initiate vesicle fusion[46]. Given this set of reports, we reasoned that divalent cations might play a similar role in our case. Among the group of divalent cations, calcium and magnesium are two candidates which enhance the rupture of membrane vesicles the most[46]. However, calcium ions can influence viral fusion of enveloped viruses such as SARS[49], so to avoid any other effects, we used Mg^{2+} instead, as that has not been reported to have impact on virus fusion. Therefore, only magnesium was studied for its effect on the formation of PD-SLBs. Additionally, since magnesium can screen

the negative charge on the PEDOT:PSS, it allows a change in the fusogenic vesicle formulation to a more physiological zwitterionic formulation. Thus, we no longer will need to use DOTAP, a synthetic lipid that is positively charged, to form an SLB. This is particularly important for the application of building a viral diagnostic platform based on the propensity of viruses to bind to their receptors that naturally exist in host cell membranes: we wish to build a platform as close the native host membrane as possible.

To test if magnesium ions contribute to the bilayer formation on PEDOT:PSS, 100 mM magnesium chloride solution was prepared and mixed with the PBS buffer so that a final concentration of 5 mM was achieved in each sample. This value was determined based on the number previously proved to promote the SLB formation on silicon-based substrates[46]. Samples with four different compositions were prepared, which were: 1 mg/mL POPC, 1 mg/mL POPC with 5 mM magnesium, 1 mg/mL POPC-peg 5k, and 1 mg/mL POPC-peg 5k with 5 mM magnesium. All samples were diluted with PBS buffer and detailed descriptions of the sample preparation can be found under method section. In order to compare the quality of the bilayers under each condition, FRAP was used to check both the amount of unruptured vesicles and the mobility of the lipids within the bilayers. Sample A, B, C and D in Fig. 9 represent the four conditions described above respectively. One thing to note here is that the two-step bilayer formation technique for pure lipids was implemented to maximize the possibility of vesicle rupture.

Like previous section, a small patch on the bilayer was photobleached with laser light and the recovery condition after 20 minutes at the same location was

recorded. Not surprisingly, without any additional treatment, POPC liposomes did not rupture on PEDOT:PSS even with the existence of external PEG (Fig. 9 A). The same behavior was observed for DOPC liposomes (not shown) during the investigation of DOTAP and layer thickness. One possible explanation for the difficulty in forming an SLB with zwitterionic lipids on PEDOT:PSS is that the hydrophilicity of the substrate is much weaker compared with the surface of a piranha treated glass. Previously, we solved this problem by introducing DOTAP that carries positive charges to increase the interaction between substrate and lipid vesicles. Therefore, similar outputs were expected for lipids that were mixed with positively-charged magnesium cations. However, as shown in Fig. 9 B, bilayers formed with this strategy only had a mobile fraction of 15%. In other words, about 15% of lipid molecules within the two-dimensional plane of SLBs were mobile, which correlates to the percentage of vesicles ruptured.

Previous studies have shown that liposomes that were prepared with PEG5k-DHPE (a.k.a. pegylated lipid) would have a larger distance from solid substrates after forming SLBs[22]. These polymer additives were also proved to facilitate vesicle fusion[25], but an exact mechanism is to be investigated. Therefore, POPC-PEG5K liposomes were made by mixing POPC with 0.5 (mol/mol) % PEG5K-DHPE and the same bilayer formation technique was used to examine the effect of pegylated lipids on the formation of PD-SLBs. Unfortunately, bilayers formed with pegylated lipids were not 100% continuous, as the mobile fraction was significantly below 1, similar to those formed using divalent cation approach. However, both strategies demonstrated a capability to improve the condition of bilayer formation and consequently a

combination of both methods may induce vesicle fusion further. Therefore, I reasoned that combining the two methods may lead to an overall higher mobile fraction through the synergy of helpful effects each strategy brings. Thus, 5 mM magnesium cations were added into POPC-peg5k solution and the same procedure was repeated on PEDOT:PSS substrates. As shown in Fig. 9 D, a significant decrease in unruptured vesicles (speckles) was detected and a mobile fraction of roughly 100% was calculated. Interestingly, the diffusion coefficients calculated for all conditions are below 0.1, which are an order of magnitude below those calculated on glass substrates. The mechanism of this phenomenon remains unknown, but one hypothesis proposed by us is the polymer cushion underneath lipid bilayers can tangle with the bottom polymeric coating, which interferes the diffusion of the fluorescence fluorophore. Fortunately, because pegylated lipids are mainly used as fusogenic vesicles to form bleb bilayers, where the percentage of the lipids as well as polymeric tails is significantly reduced. The most important feature of fusogenic vesicles for PD-bleb-SLBs is their ability to rupture on PEDOT:PSS which was successfully demonstrated above. A normal membrane fluidity was therefore expected for bleb bilayers triggered by this strategy.

1.3.3. Characterization of PD-SLBs with viral receptors incorporated

Since an approach to induce the rupture of fusogenic vesicles on PEDOT:PSS was successfully developed, next step is to build an SLB platform on the channel material with specific viral receptors incorporated. As one of the most commonly observed viruses, influenza X-31 was selected to be the first viral species characterized on our electrochemical biomimetic platform. Detailed descriptions of the

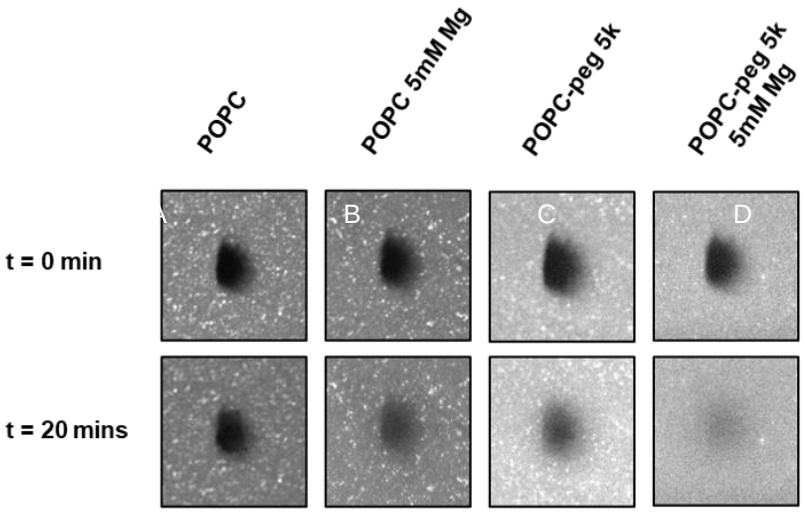

	POPC	POPCw/ 5 mM Mg^{2+}	POPC-peg5k	POPC-peg5k w/ 5 mM Mg^{2+}
Diffusivity ($\mu m^2/s$)	N/A	0.0189 ± 0.0047	0.02815 ± 0.0057	0.03180 ± 0.0074
Mobile fraction	N/A	15.0 ± 9.9%	24.2 ± 18.9%	89.8 ± 8.1%

Fig. 9 & Table 1 **Characterization of lipid bilayer formation on PEDOT:PSS films by FRAP.** Fluorescence recovery after photobleaching is shown at t = 0, 20 min of POPC, POPC with 5mM Mg^{2+}, POPC-peg 5k and POPC-peg 5k with 5mM Mg^{2+} on PEDOT:PSS. It turned out that both pegylated lipids and divalent cations are necessary in order to form a mobile SLB on PEDOT:PSS without the addition of DOTAP.

viral fusion mechanism will be discussed in next chapter, but one thing to be noted here is that the monosaccharide influenza viruses bind to is sialic acid[48], which is naturally available in the membrane of Vero E6 cells[19]. The same bilayer assembly approach was used as constructing PD-HEK-SLBs, with Vero E6 blebs replacing the HEK blebs and POPC-peg5k with 5 mM Mg^{2+} substituting the 80% DOPC/20% DOTAP. The Vero E6 blebs involved in the formation of PD-SLBs were characterized with Nanosight NS300 and the results are shown in Fig. 10 A. In addition, FRAP was used to analyze membrane mobility of PD-SLBs, and the diffusivity of the sample was calculated by fitting data into the Soumpasis equation (Fig. 10 B)[49]. As a result, the

average diffusion coefficient was determined as 0.55 ± 0.14 $\mu m^2/s$ and the mobile

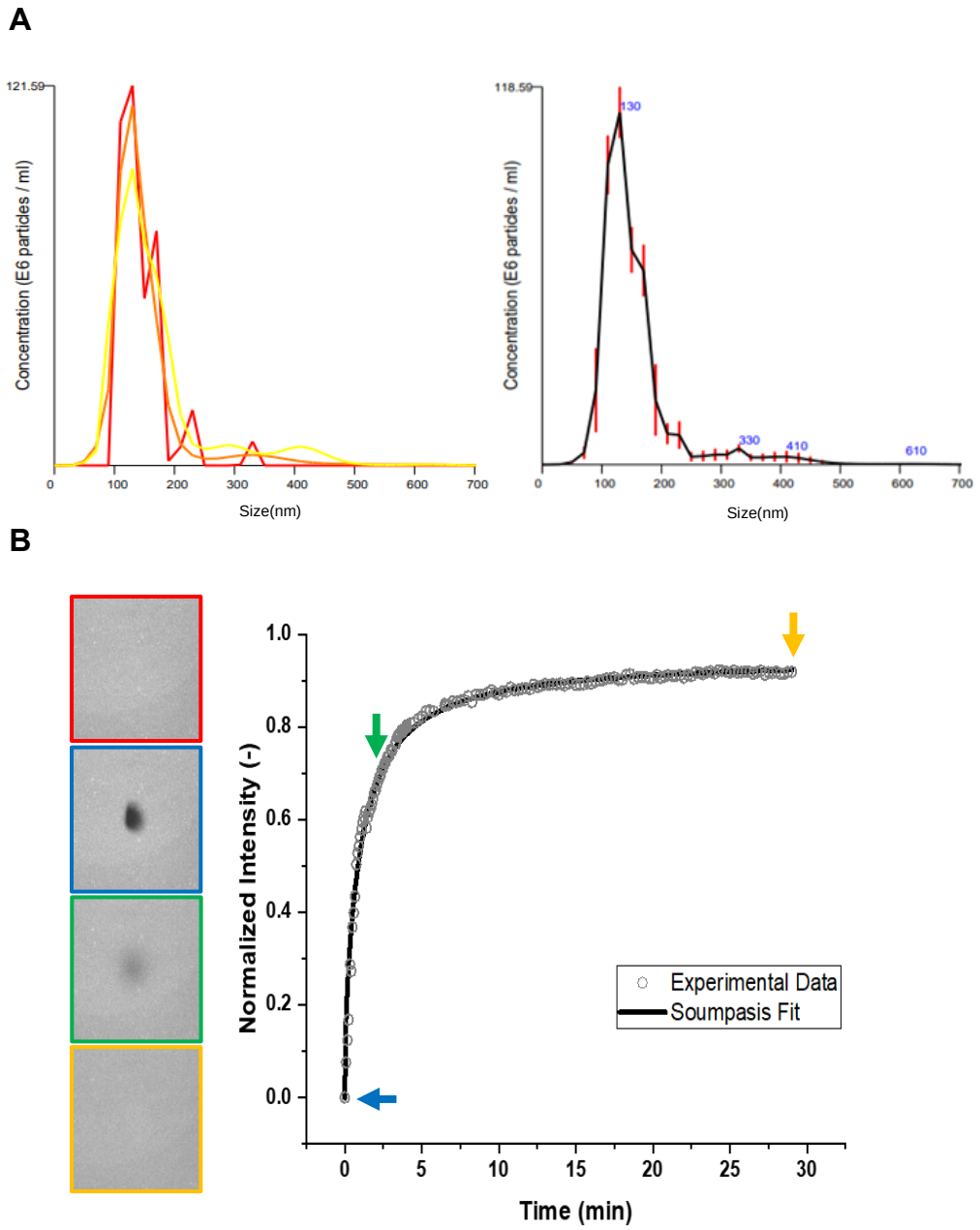

Fig. 10 **Characterization of Vero E6 cell blebs and bleb bilayers on PEDOT:PSS. (A)** The concentration and size distribution of Vero E6 solution used for the formation of PD-SLBs were determined using Nanosight NS300. Consequently, the concentration of the bleb solution was determined to be 4e8 ± 2.57e7 particles/mL and the size distribution was determined to be 144.9 ± 7.3 nm. **(B)** The mobility of PD-Vero E6-SLBs were characterized using FRAP. *Left:* Microscopic images of fluorescence recovery after photobleaching. Right: Normalized intensity vs. time at the photobleached spot. The data were fitted to Soumpasis equation in order to determine the fluidity of the bilayer.

fraction was calculated to be 98.4 ± 2.7%, both of which are the same order of magnitude as their glass counterparts where the diffusivity and mobile fraction were characterized to be 0.34 ± 0.01 $\mu m^2/s$ and 99.8 ± 0.32% respectively. Now that a biomimetic platform that mimics the host cell membrane of influenza X-31 viruses is successfully constructed on PEDOT:PSS with a diffusivity that is physiologically meaningful, next step is to determine the orientation of viral receptors on the bilayer and examine if viral fusion would occur on such platform.

1.4. Conclusion

To investigate the use of an organic electrochemical transistor that can monitor interactions between enveloped viruses and host cell membranes, supported lipid bilayers need be constructed on the polymer channel, PEDOT:PSS, in the transistor. Previously, our group developed a strategy to incorporate membrane components into SLBs using cell blebs on the glass substrate[19], but the same output was difficult to repeat on PEDOT:PSS due to electrostatic interactions as well as unfavorable surface smoothness. In this work, we implemented different approaches to induce vesicle fusion on the polymer substrate, which include adjusting polymer thickness, mixing magnesium cations with zwitterionic lipids, inserting PEG cushions underneath bilayers, and adding external PEG. Our use of PEGylated lipids and divalent cations in the rupture vesicles reduced the electrostatic interactions interfering vesicle fusion and provided enough space for the vesicles to deform. Meanwhile, the existence of external PEG generated a crowded macromolecular environment that pushed vesicles towards each other and caused a strong osmotic shock that promoted vesicle fusion on the surface. Together, these techniques led to the formation of

continuous Vero-SLBs with normal R18 fluidity of around 0.55 $\mu m^2/s$ and minimal unruptured vesicles on the surface. With this platform built on PEDOT:PSS, further characterization can be done including determining the membrane protein orientation (critical to ensure the binding site is the right side up), single particle tracking of enveloped viruses, and electrochemical impedance spectroscopy.

1.5. Acknowledgement

The author would like to thank the National Science Foundation and the Defense Advanced Research Projects Agency for supported the work presented in this Article. I would like to acknowledge Chih-yun Hsia, former PhD student in our group, for bringing up the idea of using osmotic shock to induce vesicle rupture on PEDOT:PSS in her previous publication “Supported Lipid Bilayer Assembly on PEDOT:PSS Films and Transistors”. In addition, I would also like to acknowledge Han-yuan Liu for his suggestion towards using external PEG which plays a critical role in this project and Tiffany Tang for helping me characterize bleb size.

Chapter 2

Viral fusion kinetics of H3N2 influenza virus into PD-SLBs

2.1. Introduction

Influenza A viruses are enveloped, single-stranded, negative-sense RNA viruses that cause seasonal epidemics of disease in the United States almost every year[5]. The influenza A hemagglutinin (HA) glycoprotein, a Class I fusion protein, mediates the binding of a flu virus to its sialic acid receptors and regulates the merging of the virus envelope with its target membrane. A detailed illustration of a common viral fusion pathway of enveloped viruses with Class I fusion proteins is shown in Fig. 11[50]. Specifically, for an influenza A virus, after binding to the sialic acid moieties on its target cell membrane, it is taken up via clathrin-mediated endocytosis and internalized by an endosome. Afterwards, low pH (5-4.5) inside of the late endosomes triggers major conformational changes in HA proteins and thrusts fusion peptides within the proteins into the endosomal membrane. Subsequently, three neighboring HA trimers move to the fusion spot and refold together to bring the viral membrane to the inner leaflet of the endosome. This initiates a hemifusion event and further merging of the inner leaflets results in the formation of a fusion pore so that viral genome can be released into the cytosol of the infected cell.

Previously, we and other research groups have successfully employed single particle tracking (SPT) technique based on TIRFM to study the fusion kinetics of influenza viruses to various cell membranes[18,20,53]. However, to extend the application of these platforms to include viral diagnosis based on genome detection (Background

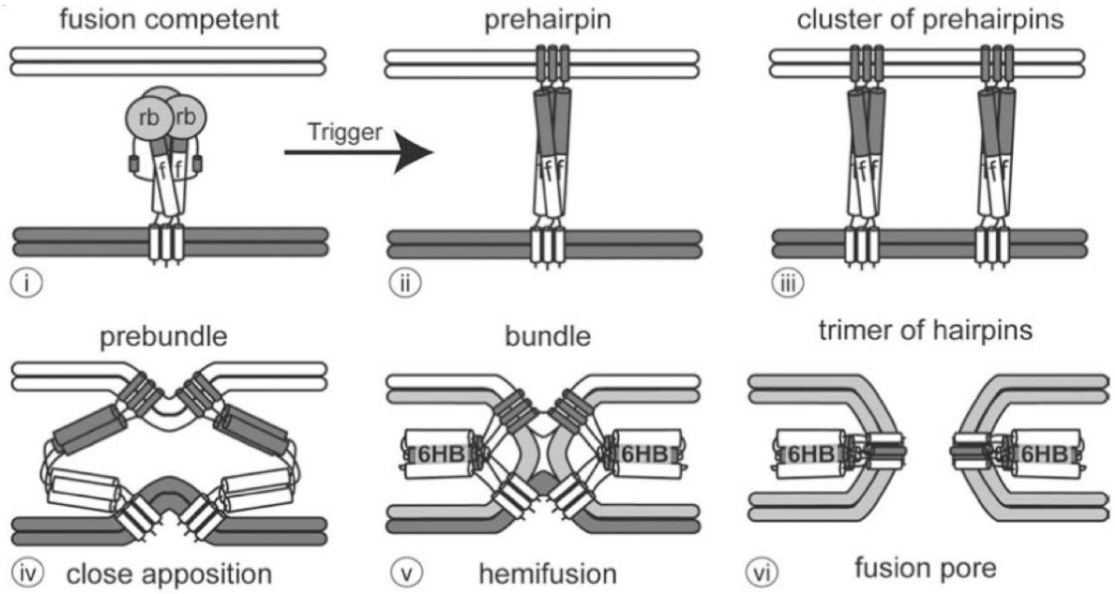

Fig. 11 **An illustration of the trimer-of-hairpins pathway of Class I fusion proteins.** A common Class I fusion protein contains a receptor binding subunit (rb) and a fusion subunit (f). (i) The receptor binding subunit at the top of the fusion protein binds to its receptor to initiate the fusion process. (ii) After triggering, the protein converts to a prehairpin intermediate, inserting the fusion peptide into the host membrane. (iii) Several membrane-embedded proteins cluster together near the fusion site. (iv-vi) Fusion proteins refold to drive the fusion of two membranes and the formation of a fusion pore. Adapted from White et al.

Information), the common setup is not adequate because genetic materials cannot be monitored using fluorescent microscopes. This application is further limited since substrates used in such platforms are electrically insulated, which prevents the identification of charged viral genomes using electrical means. PD-SLBs, a biomimetic platform constructed on PEDOT:PSS using natural cell blebs, PEGylated lipids, divalent cations, and external macromolecules, raise the possibility to detect and identify enveloped viruses while monitoring their fusion to the target membranes. Nevertheless, viral fusion experiments on PD-SLBs have never been conducted before and the compatibility of the platform with such characterization is to be determined. One key factor for a successful *in vitro* viral fusion analysis on PD-SLBs is the orientation of viral receptors that are incorporated into the bilayers by rupturing cell

blebs. Due to the two-dimensional structure of the model membrane, receptors that are facing towards the underneath polymeric coating cannot function as a binding site for enveloped viruses that are available on the other side of the bilayer. Our previous tests on protein orientation for SLBs constructed on glass cover slides all indicated a "parachuting" rupture mode for cell membrane vesicles with membrane proteins facing outwards (Fig. 5&12)[22,30,54], but due to the presence of lipid-PEDOT substrate interactions, an exact rupture mechanism for PD-SLBs remains unknown.

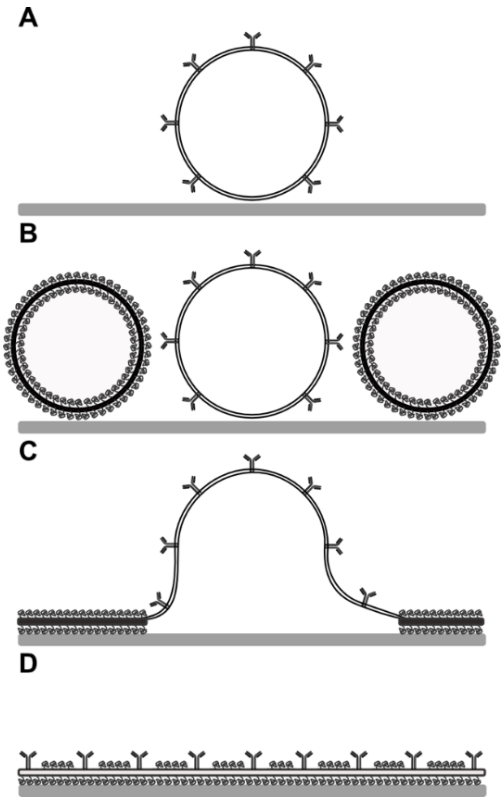

Fig. 12 **Illustration of PEGylated bleb bilayer formation on glass slides.** Cell blebs (white circle) are deposited onto the glass substrate and PEGylated fusogenic vesicles (black lipid circle with brown polymer cushion) are added. Fusogenic vesicles rupture spontaneously on hydrophilic surface which induces the rupturing of adjacent blebs. A "parachuting" rupture mode was determined from an enzymatic analysis.

In the first part of this thesis, I investigated the rupture mechanism of Vero E6 blebs, a natural carrier of influenza A viral receptors[51], on PEDOT:PSS. Now I will examine the protein orientation in PD-VeroE6-SLBs. This involves transfecting two different fluorescent proteins: glycophosphatidylinositol yellow fluorescent protein (GPI-YFP) and P2X2 receptor fused to a neon green fluorescent protein (P2X2-neon) onto the membrane of Vero E6 cells, which have cleavage sites that when exposed to a protease will be removed from the protein. In this way, I can monitor the fluorescence signal change with a microscope after adding enzymes to see

when the fluorescent subunits are removed. In addition, because the YFP of GPI-YFP and neon of P2X2-neon are exposed to the extracellular and intracellular environment respectively[31], a combination of the two proteins excluded the possibility of a false orientation determination resulted from enzymes passing through defects in the membrane to cleave proteins that were originally underneath. It is important to note that this assay is possible because the PEDOT:PSS layer is transparent and thus fully compatible with fluorescence microscopy. Consequently, the orientation of both types of membrane proteins was determined to be facing predominantly outwards, indicating the same "parachuting" rupture mode as previously reported on glass substrates and ensuring the receptor proteins on the PEDOT layer where in fact facing in the correct orientation necessary for virus binding.

In the second part of this chapter, a series of experiments were conducted to determine the compatibility of PD-SLBs to serve as a platform for observing viral fusion. Two types of SLBs were constructed following the strategy developed in last chapter: one was PD-VeroE6-SLB which maintains the natural components of a target cell membrane by rupturing cell blebs using zwitterionic lipids along with other stimuli. The other one was a customizable synthetic lipid bilayer[16], containing a mixture of zwitterionic lipids, cholesterol, total ganglioside extract (TGE) whose composition can be adjusted to characterize the content of each component on viral fusion. TGE possesses glycolipids that connect to sialic acid groups, necessary for influenza virus binding. Both types of SLBs incorporate Oregon green DHPE, which is a pH sensitive fluorophore that no longer fluoresces in the presence of an acidic environment. Thus, Oregon green DHPE serves as a visual indication of when the

bound viruses are acidified for fusion[52,55]. The interval of time between the pH drop and hemifusion for each individual virion is defined as hemifusion lag time, from which the hemifusion kinetics of the virus was calculated. We demonstrate here the use of PD-SLBs to study the fusion kinetics of influenza A viruses for the first time and compare them with those previously analyzed on glass substrates to test its performance.

2.2. Materials and methods

2.2.1. Cell lines and plasmids

Vero E6 cells used in experiments were obtained from the American Type Culture Collection and grown in Dulbecco's modified Eagle's medium (DMEM; CellGro) supplemented with 10% heat inactivated fetal bovine serum (Gibco), penicillin streptomycin solution (5000 I.U./mL Penicillin and 5000 μg/mL streptomycin; CellGro) and 1% HEPES buffer (CellGro) in a 37 °C, 5% CO_2 incubator (ESCO).

The pYFP-GPI-N1 plasmid was obtained from the Baird/Howlawka research group at Cornell University and was used to transfect glycophosphatidylinositol (GPI) anchored yellow fluorescent protein on the cell plasma membrane with the yellow fluorescent protein facing outwards. The pINR3-Neon-THR-P2X2 plasmid was designed following the method developed by Richards et al.[22] by combining a thrombin cleavage site (Gly-Leu-Val-Pro-Arg-Gly) with the full length mouse P2X2 protein (GI:258679504). It was used to transfect P2X2-neon in the cell membrane with the neon green protein encapsulated in cytosols.

2.2.2. Virus labeling

Influenza X-31 (H3N2) viruses were purchased from Charles River Laboratories with a hemagglutinin concentration of 2 mg/mL and Octadecyl rhodamine B chloride (R18) was used to label virus membranes. In this case, 5 μL of virus and 0.5 μL of R18 were added to 250 μL of PBS buffer. The mixture was then sonicated in a water bath for 30 min. Afterwards, a G-25 spin column was used to remove unbounded R18 from the solution by centrifuging for 2 min at 735 g. Afterwards, phosphate buffered saline (PBS) buffer (5 mM NaH_2PO_4, 5 mM Na_2HPO_4, 150 mM NaCl at pH 7.4) buffer was added into the mixture so that the total volume became 800 μl.

2.2.3. Liposome preparation

Oleoyl-2-palmitoyl-sn-glycero-3-phosphocholine (POPC), 0.5% (mol/mol) 1,2-dipalmitoyl-sn-glycero-3-phosphoethanolamine-N-[methoxy(polyethylene glycol)-5000] (PEG5000-PE), 1,2-dioleoyl-sn-glycero-3-phosphocholine (DOPC), and 1,2-dioleoyl-3-trimethylammonium-propane (DOTAP) were purchased from Avanti Polar Lipids and Oregon green DHPE was ordered from Molecular Probes. The liposomes were prepared in glass vials by mixing a certain amount of lipids in chloroform (Sigma) to achieve the desired composition ratio. The vials were placed under a stream of high purity nitrogen gas for 5 minutes and then desiccated for 3 hours to evaporate any remaining chloroform. Sufficient amount of phosphate buffered saline (PBS) buffer was then added to rehydrate the dried lipid films so that the concentration of liposomes became 2 mg/mL. The lipid mixture was then frozen overnight at -20 °C, thawed next day and extruded using a 50 nm membrane for at

least 15 times. Three lipid compositions were used in this work, which are 99.4% POPC/0.5% PEG5k/0.1% Oregon green DHPE (mol/mol), 80% DOPC/20% DOTAP (mol/mol), and 36.3% DOPC/36.3% POPC/18.2% cholesterol/4.5% total ganglioside extract (TGE)/4.5% PEG5K/0.1% Oregon green DHPE. After preparation, liposomes were stored at 4 °C for at most one week until use.

2.2.4. Membrane bleb preparation

10 mL of 5.0×10^5 cells/mL of Vero E6 cells were seeded in a 10 cm Petri dish (Corning) and incubated in a 37 °C, 5% CO_2 incubator for 24 hr. If necessary, transfections were performed by adding 15 μL of Turbofect (Thermoscientific) and 10 μg of DNA plasmid in the dish, following by another 24 hr incubation under the same condition. After this, cells were rinsed with GPMV buffer (2 mM $CaCl_2$, 10 mM HEPES, 150 mM NaCl at pH 7.4) and subsequent blebbing was performed by adding 4 mL of blebbing buffer which consists of 2 mM dithiothreitol (Sigma) and 25 mM formaldehyde (Sigma) in GPMV buffer. The cells were incubated for 2 hr at 37 °C and the media was then transferred to a 15 mL ultracentrifuge tube. The tube was placed on ice for 15 min to remove cell debris, after which the top supernatant was carefully pipetted and transferred to a new tube.

2.2.5. PEDOT:PSS slide preparation

Glass slides (25 × 25 mm No. 1.5, VWR) were cleaned with piranha solution (30% (v/v) H2O2 (Sigma 50 wt%) and 70% (v/v) H_2SO_4 (BDH)) for 10 min and then rinsed for 30 min under 18.2 MΩ-cm water (ELGA Purelab Ultra, Woodridge, IL). Slides were kept immersed under 18.2 MΩ-cm water for no longer than 3 days until use. PEDOT:PSS dispersion was prepared by mixing 5% (v/v) ethylene glycol

(Sigma-Aldrich), 0.002% (v/v) DBSA (Sigma-Aldrich) and 1% (w/w) GOPS (Sigma-Aldrich) with Clevios PH 1000 (Heraeus Clevios GmbH). The dispersion was sonicated in a sonication bath for 30 min to reduce aggregations before use. Glass slides were then dried with nitrogen, O_2 plasma cleaned at 150W for 2 min and coated with the PEDOT:PSS dispersion by spin-coating at 4000 rpm for 30 s. After a homogeneous film covered the entire surface, substrates were baked at 140 °C for 1 h, followed by 4 h immersion under 18.2 MΩ-cm water.

2.2.6. Size and concentration characterization for influenza A viruses

Nanosight NS300 (Malvern) was used to determine the size distribution and concentration of cell blebs in GPMV buffer. Before characterization, samples were diluted 1 to 100 using PBS buffer.

2.2.7. Fabrication of microfluidic devices

The production of microchannel silicon mold using soft lithography followed methods previously published[19,21,53]. A pattern was used as a mold for microfluidic devices, which contained six trenches that were 70 μm deep, 135 μm wide and 1.5 cm long with 100 μm spacing between each channel. A microfluidic device was prepared by mixing a 10:1 (elastomer:crosslinker) mixture of Sylgard 184 (Dow Corning), degassing in a desiccator, and then curing on the mold under 80 °C for 3 h to form Polydimethylsiloxane (PDMS) with six channels as designed. The mold was coated with chlorotrimethylsilane (Sigma-Aldrich) via vapor deposition to facilitate PDMS detachment. Before assembling the microfluidic device with a PEDOT:PSS substrate, both the PDMS and the PEDOT:PSS substrate were treated with oxygen plasma using a Harrick Plasma Cleaner (Model # PDC-32G) at a pressure of 750 millitorr on the

"high" setting for 15 s. Finally, the two pieces were affixed together tightly and annealed under 80 °C for 10 min.

2.2.8. Supported lipid bilayer formation in microfluidic channels on PEDOT:PSS substrates

After the annealing of a microfluidic device with a PEDOT:PSS substrate, a solution containing a 1:1 dilution Vero E6 blebs in GPMV buffer (for bleb bilayer) or 1 mg/mL liposome mixture with 5 mM Mg^{2+} in PBS buffer (for synthetic lipid bilayer) was drawn into the microfluidic channel at a flow rate of 100 μL/min for 1.2 min. The vesicles were then incubated on the PEDOT:PSS surface for 15 min and the microfluidic channel was rinsed with the same type of buffer as the membrane vesicles at 100 μL/min for 1.2 min. For bleb bilayer, a solution of 1 mg/mL fusogenic liposomes with 5 mM Mg^{2+} was drawn into the channel at 30 μL/min for 4 min, incubated for 15 min, and channel was rinsed with PBS buffer at 100 μL/min for 1.2 min. For synthetic lipid bilayer, no additional fusogenic vesicles were added. The formation of a supported lipid bilayer was induced by drawing a solution of soluble polyethylene glycol 8000 (30% w/v PEG-8000 in PBS buffer, VWR) at 100 μL/min for 1.2 min into the channel for both cases and incubated for 60 min. Finally, the microchannel was rinsed with PBS buffer at 100 μL/min for 1.2 min to remove any excess liposomes.

2.2.9. TIRF microscope configuration

Single virion fusion assays were conducted using total internal reflection fluorescence microscopy (TIRFM) with an inverted Zeiss Axio Observer.Z1 with a α Plan-Apochromat 100× oil objective with a numerical aperture (NA) of 1.46. Index-

matching immersion oil (Carl Zeiss, Inc.) was added to the objective to couple the glass bottom of the microfluidic device to the objective. Laser light with 561 nm and 488 nm excitation wavelengths were used to excite R18 in virus membranes and Oregon-green in supported lipid bilayers simultaneously. In order to adjust the angles of incidence so that total internal reflection was achieved at the glass/water interface, a laser TIRF 3 slider (Carl Zeiss, Inc.) was used so that the angle was around 68°. In this case, evanescent waves of approximately 100 nm thickness were created. Since the viral binding and fusion occurs within the region of evanescent waves, background noise generated from unbound viruses in the bulk solution was reduced significantly.

2.2.10. Enzyme accessibility assays for the determination of protein orientation in PD-SLBs

300 U/mL of thrombin (Sigma) and 100 μg/mL of proteinase K (Ambion) were used to test the accessibility to the N-terminus neon domain of P2X2-neon and the YFP domain of the GPI-YFP. PD-SLBs were assembled in a PDMS well as discussed in previous chapter, and enzymes were added into the solution on top of the PD-SLBs. Images of various spots on the bilayers were recorded at 5 min intervals and the fluorescence signal loss was recorded as cleaved fluorescent proteins diffused out of the evanescent fields (Fig. 13). As a negative control, fluorescence signal loss due to photobleaching was analyzed by counting the reduction in the number of particles on the same bilayer during the same time interval without adding any enzyme. In addition, due to the conjugation structure inside of PEDOT:PSS, their autofluorescence can be captured by fluorescence microscope under the same experimental set up. To test the effect of enzymes on the autofluorescence of

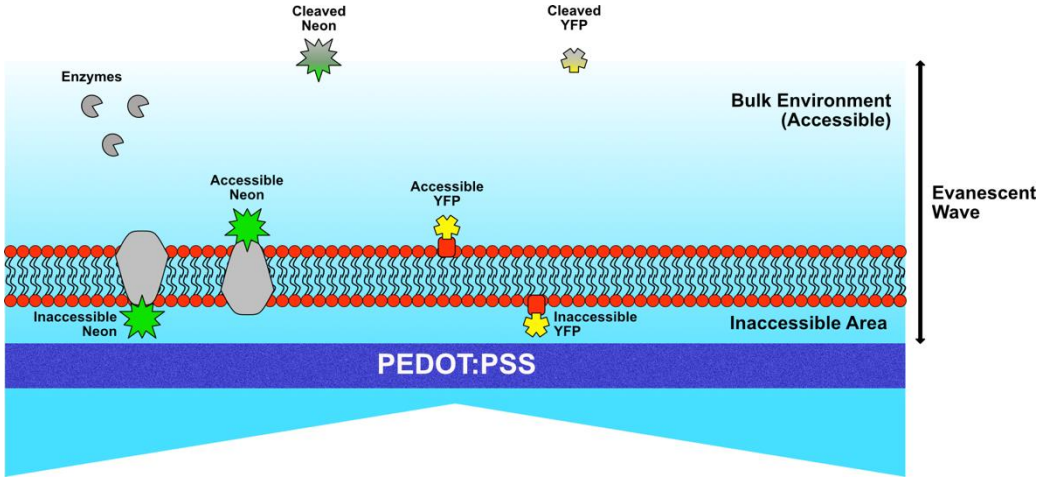

Fig. 13 **Enzyme accessibility assay for protein orientation.** P2X2-neon (transmembrane protein in gray) and GPI-YFP (peripheral membrane protein in red) are shown on a PD-SLB (red bilayer). Both neon green protein and yellow fluorescent protein can be excited by the evanescent wave generate from a 488 nm laser light, emitting green and yellow color respectively. Enzymes (thrombin for P2X2-neon and proteinase K for GPI-YFP) are added into the bulk environment and they can cleave fluorescent proteins that are on top of the bilayer. Once the cleaved proteins diffuse out of the evanescent wave, they no longer generate fluorescent signal, which results in a signal loss under fluorescent microscopes. This allows the determination of protein orientation on PD-SLBs.

PEDOT:PSS, 100 μL of PBS buffer was added into each PDMS well on PEDOT:PSS substrates and one type of enzyme was added into the PDMS well each time. Images of various spots on PEDOT:PSS were recorded at 5 min intervals.

2.3. Results and discussion

2.3.1. Orientation of membrane proteins in PD-SLBs

The availability of specific viral receptors on the target cell membrane is critical for enveloped viruses to fuse into the membrane and release their viral genome. Correspondingly, the viral diagnostic platform that we are developing leverages the natural propensity of enveloped viruses to fuse their membranes with host membranes to insert their viral genome. The detection and identification will be made based on the electrical signal change induced by the additional materials from

the merging of viral envelopes and by the release of charged genome from fused virions. Due to the two-dimensional structure of an SLB, only components on the upper leaflet of the bilayer will be available for viruses to interact with. Therefore, determining the rupture orientation of cell blebs, the only source of viral receptors during the formation of PD-SLBs, is crucial for the application of a viral sensor development.

However, proposing a general rupture model for cell blebs is difficult due to the complicated interactions of the membrane vesicles with their neighboring molecules (e.g. liposomes and PEG8K) as well as with the charged substrate underneath. Furthermore, observing the real-time rupture of cell blebs is also challenging, as there are no techniques capable of doing so. Fortunately, previous studies[22,30,54] demonstrated a close relationship between the orientation of membrane proteins with the rupture direction of cell blebs; these studies show a significant consistency between protein orientation in SLBs and that in natural cell membrane, indicating a "parachuting" rupture mode for blebs (Fig. 12). Ideally, the orientation of proteins in PD-SLBs should be predominantly the same as that in natural cell membranes. This requires the components on the upper leaflet of the bilayer maintain the same as those originally on the outer cell membrane.

To confirm this, two different fluorescent proteins, GPI-YFP and P2X2-neon, were transfected on the Vero E6 cell membrane before inducing the blebs. Like viruses, enzymes can only access to protein domains that are located on top of the membrane. For GPI-YFP, the enzymes added were proteinase K which can cleave any protein domains that are exposed to the bulk environment[22]. In this case, the YFP can

only be released from its membrane if the protein is on the upper leaflet of the SLB, resulting in a fluorescence signal loss under microscope. Considering GPI-linked proteins are peripheral membrane proteins, this indicates the natural orientation of cell membrane is maintained within the SLB. Conversely, for transmembrane protein P2X2-neon, the neon fusion protein originally remains in the lumen of the cell. If PD-SLBs have the same orientation as cell membranes, the thrombin cleavage site would not be exposed to enzymes and no significant change in fluorescence signal would be observed. To control for photobleaching effects, one additional sample was prepared on the same substrate without enzyme and the fluorescence signal change was monitored for the same duration of time. Moreover, the total number of autofluorescence was recorded for each experiment to avoid data misinterpretation.

As shown in Fig. 14, a significant drop in fluorescence signal was observed for GPI-YFP with approximately 100% effective signal loss, where effective signal loss is defined as:

$$\text{E.S.} = \frac{\text{change in particle number}}{\text{initial particle number - average autofluorescence number}} \times 100\%$$

Since the result of GPI-YFP shows a substantial change in the signal, additional sets of experiments were conducted to check the effect of proteinase K on the autofluorescence of PEDOT:PSS, which was measured by adding the same amount of enzymes on the substrates without any membrane materials. The green line marked with empty squares illustrates the change in autofluorescence signal of the conjugated polymer after adding proteinase K. No obvious variation was observed after 20 min which indicates the signal loss in GPI-YFP came mainly from protein cleavage. In

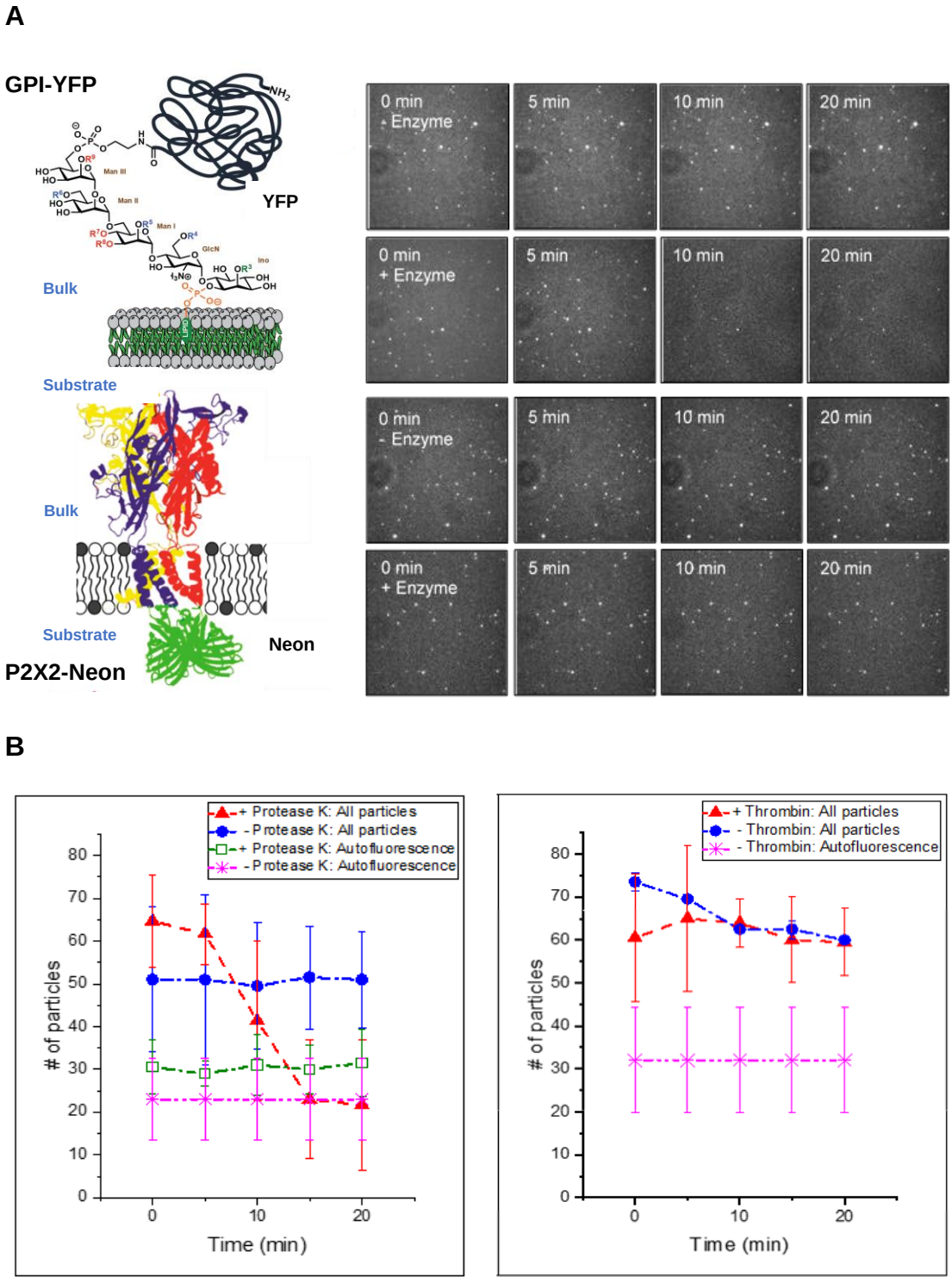

Fig. 14 **Determination of protein orientation through fluorescence accessibility assays. (A)** Microscopic images demonstrating changes in the number of fluorescent proteins +/- enzymes. **(B)** After adding proteinase K, the signal change for GPI-YFP (left red) demonstrates a sharp decrease. However, the same phenomenon was not observed for P2X2-Neon after the addition of thrombin (right red). This indicates that the outer leaflets of cell blebs are predominantly facing upwards in PD-SLBs.

contrast, approximately no effective signal loss was detected for P2X2-neon after the

same time interval. This proves the overall quality of PD-SLBs as thrombin would otherwise go through defects in the bilayers to cleave neon green proteins underneath[31]. Combing the results of both proteins, we conclude that for both GPI-YFP and P2X2-neon, bleb bilayer orientation matches that of the cell and a "parachute" mechanism is proposed for the bilayer formation on PEDOT:PSS (Similar to the one shown in Fig. 12). In addition, a success in cleaving protein domains in GPI-YFP proves that the external PEG added to induce the rupture of fusogenic vesicles was either removed via thorough rinsing or did not impact the ligand's ability to bind to their receptors. Even though an exact conclusion cannot be made for the formation mechanism of PD-SLBs, the platform has successfully demonstrated for its potential for analyzing viral fusion.

2.3.2. Comparison of the effects of different bilayer compositions on the viral fusion of influenza X-31 viruses to PD-SLBs

The influenza viruses used in single particle tracking were labeled with a lipophilic dye, R18, which quenches at high concentration[18,19,23]. Such quenching of fluorescence is alleviated when the outer leaflet of viral membrane merges with the upper leaflet of an SLB during a hemifusion event. This is because the concentrated dyes can now diffuse into the supported bilayer and are no longer be concentrated. The diffusion of the dye can be monitored under TIRFM and is visualized as a "firework" like burst which indicates a successful hemifusion event. However, this requires the viruses to be localized within the 100 nm evanescent wave generated from total internal reflection (Fig. 15 A). Therefore, before conducting SPT to calculate the fusion kinetics of influenza X-31 viruses to PD-SLBs, size characterization was

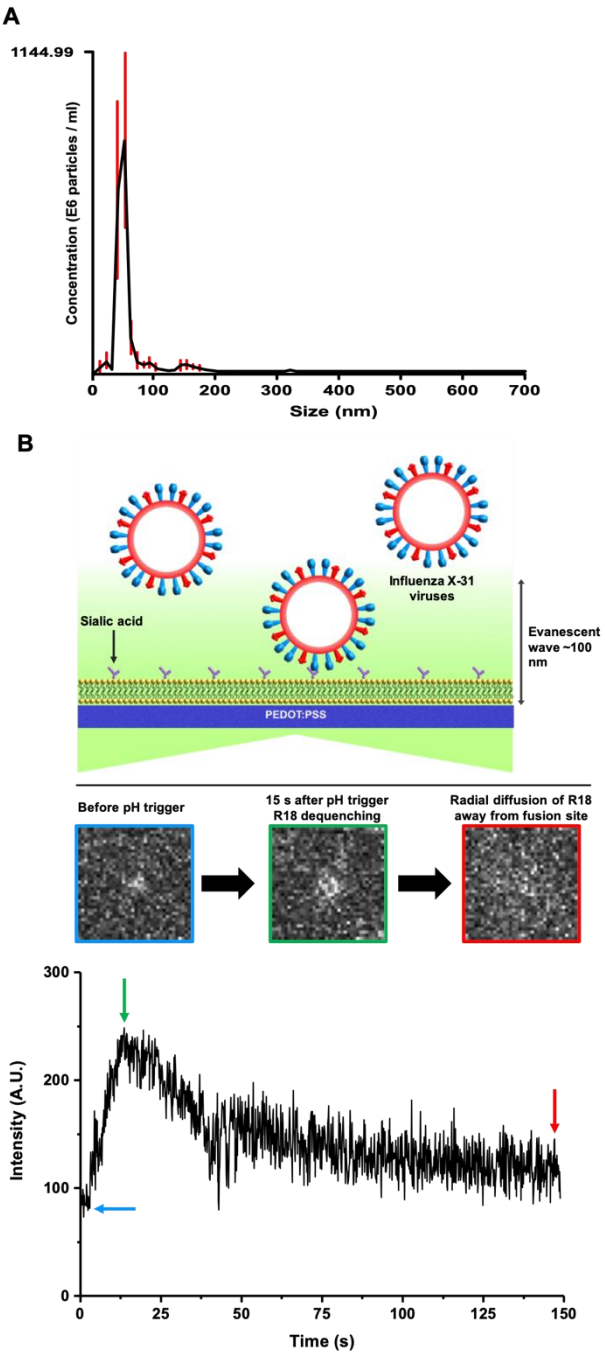

Fig. 15 **Single virion tracking on PEDOT:PSS using TIRFM. (A)** The size and concentration of influenza X-31 viruses were characterized using Nano-sight NS300 to check their compatibility with TIRFM. The size of the viruses was determined to be 56.8 +/- 6.3 nm which is within the range of an evanescent wave. In addition, the concentration of the virus stock was determined to be 1.95e9 +/- 6.34e8 particles/mL. This was used to determine the amount of fluorophore to label viruses. **(B)** *Top:* Three influenza X-31 viruses are shown with their membranes labeled with fluorescence dye R18. The center virus is bound to sialic acid (purple), which stabilizes it within the evanescent wave generated from total internal reflection. Note that only the middle virus would be observed under TIRFM in this case. *Bottom:* sample images of one influenza X-31 virion labeled with R18 fusing into PD-SLBs after acidification. An intensity trace was plotted to obtain the lag time to hemifusion (green).

performed using Nanosight NS300 to determine The mean diameter of the viruses was determined to be 56.8 nm with a standard deviation of 6.3 nm. The thickness of a single-layer SLB was reported to be around 4 nm[52], indicating the majority of bound viruses were localized within the 100 nm evanescent wave after binding to sialic acids. This enabled the fluorophore inside of virus membranes to be excited by the laser light and fusion events could therefore be monitored with TIRFM.

To create a platform for viral fusion analysis, microfluidic devices with multiple channels were assembled on PEDOT:PSS substrates and membrane materials were coated on the bottom of each channel. Individual virion fusion measurements were conducted using TIRFM and a typical hemifusion event recorded using fluorescence microscopy is shown in Fig. 15 B[18,23]. For this study, six different experimental setups were designed to test the compatibility of the biomimetic platform with single particle tracking techniques established in the group (Fig. 16). These conditions examined if viral fusion would happen when 1) nothing was absorbed, 2) only Vero E6 blebs that would not rupture spontaneously were absorbed, 3) pure POPC-PEG5K lipids without receptors were ruptured, 4) Vero E6 blebs with DOPC/DOTAP were ruptured, 5) POPC-PEG5K lipids with TGE extracts that contain viral receptors were ruptured, and 6) Vero E6 blebs with POPC-PEG5K were ruptured, all on PEDOT:PSS surfaces. External PEG solution as well as divalent cations were applied to all conditions above, with the exception of the DOPC/DOTAP case, in which only external PEG was added, to control the same experimental conditions.

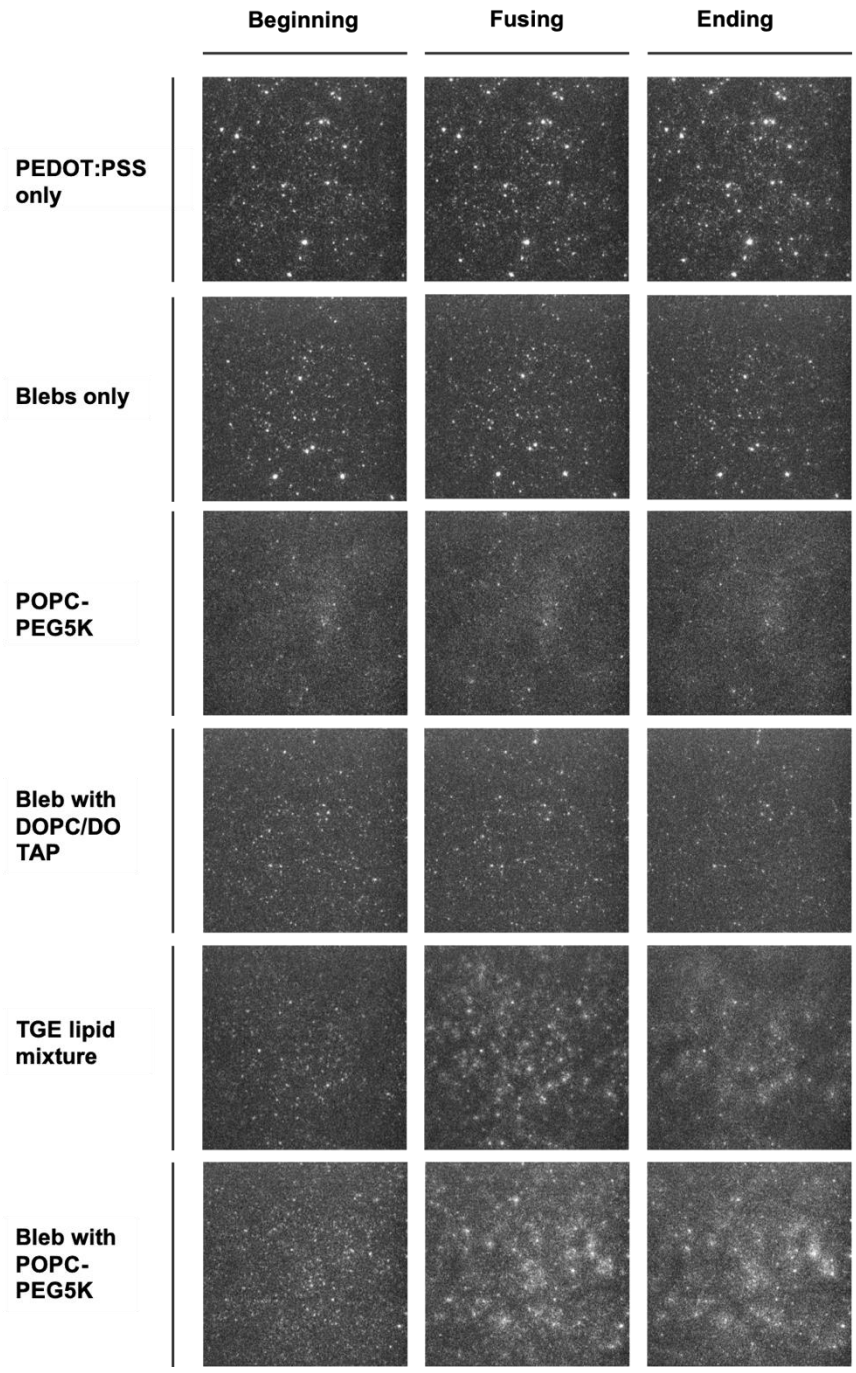

Fig. 16 **Microscopic images of hemifusion of influenza X-31 viruses to various PD-SLBs after acidification at pH=4.5.** Adequate amount of viruses were flowed into a microfluid channel where a PD-SLB was coated (if any) on the bottom surface. After binding, buffer A with pH=4.5 was flowed into the channel to trigger hemifusion of the viruses (shown above). Oregon green DHPE was incorporated into the SLB to indicate the beginning of acidification. As a result, fusion was only observed on PD-SLBs that are continuous, have receptor incorporated, and have no aggregation on the surface (an opposite example is bleb with DOPC/DOTAP with DOTAP aggregating on the surface).

As expected, viruses that bound to plain PEDOT:PSS substrates could not fuse after flowing acidic (pH = 4.5) buffer into the channels, because neither receptors nor mobile membranes were available for them to interact with. This experiment is important because it proves that charged fluorophores inside of viral membranes cannot spread out onto PEDOT:PSS coatings, as such event could resemble a typical hemifusion activity as recorded by TIRFM. Similarly, trivial numbers of fusion events were observed after acidifying viruses that bind to either intact Vero E6 blebs, or continuous POPC-PEG5K bilayers without any receptors on PEDOT:PSS. The observations confirm that both viral receptors and continuous SLBs are required to record a viral fusion event using TIRFM successfully. Afterwards, the formation of Vero E6 bleb bilayer on PEDOT:PSS was triggered by 80% DOPC/20% DOTAP following the three-step strategy developed in last chapter. Barely any fusion was observed which proves our hypothesis that the existence of positively charged lipids can interfere viral fusion into PD-SLBs. Finally, two types of bilayers were constructed using Vero E6 blebs or TGE extracts that contain sialic acids, both of which were formed with POPC-PEG5K liposomes, 5 mM Mg^{2+} and soluble PEG solution. As a result, hemifusion events were clearly monitored using TIRFM in the form of fluorescent diffusion (bottom two rows in Fig. 16) in both scenarios. This demonstrates both the continuity of SLBs in the biomimetic platform we developed and had a successful incorporation of viral receptors with proper orientation.

2.3.3. Characterization of influenza X-31 hemifusion kinetics to PD-SLBs using single-virion tracking

Now that PD-SLBs with normal fluidity, high percentage of mobile fraction, proper protein orientation, and decent compatibility with two-dimensional viral fusion analysis have been designed, one last factor to be characterized before conducting any electrical measurements was the viral fusion kinetics on these platforms. Considering the difference in surface properties between glass and PEDOT:PSS, we expected slightly different fusion kinetic values on PEDOT:PSS than on glass. Specifically, the hemifusion rate constant and number of fusion proteins involved can be calculated by fitting lag times of every hemifusion event, which is defined as the time interval between pH drop and hemifusion for each individual virion, into a gamma distribution[21], shown below:

$$P_H(t) = \frac{k_1{}^N t^{N-1}}{\Gamma(N)} e^{-k_1 t} \quad (2)$$

where P_H represents the hemifusion probability density, k_1 represents the hemifusion rate constant, N represents the number of independent transitions which was interpreted as the total number of HA proteins involved in one hemifusion event[21], and t represents the lag time to hemifusion.

The hemifusion frequencies of native influenza X-31 viruses fusing into Vero E6 bleb bilayers and TGE lipid bilayers on PEDOT:PSS are plotted in Fig. 17 against those on glass cover slides, and the results of fusion kinetics are summarized in Table 2. Independent of surfaces, viral fusion happens faster on TGE lipid bilayers, where k_1 is equal to 0.53 and 0.29 for PEDOT:PSS and glass respectively, than that on bleb bilayers, where k_1 was reported to be 0.39 and 0.18 accordingly. A potential explanation can be attributed to the cholesterol content in the bilayers. TGE bilayers

have 20% cholesterol, whereas bleb bilayers have less, as the membranes used to make blebs have 20%-30% cholesterol, which are diluted when using fusogenic vesicles to form the bilayer[56]. Cholesterols have been demonstrated to facilitate the fusion of various types of viruses[55] and to stabilize the fusion pore after formation[56]. Meanwhile, when comparing TGE and bleb bilayers on PEDOT:PSS with their respective conditions on glass substrates, it is observed that the hemifusion rate constants are higher in both cases on the polymer surface compared with glass. Due to the trend consistency in both scenarios, we hypothesize that the bilayer-substrate interaction was the main cause for the difference in hemifusion rate constants between

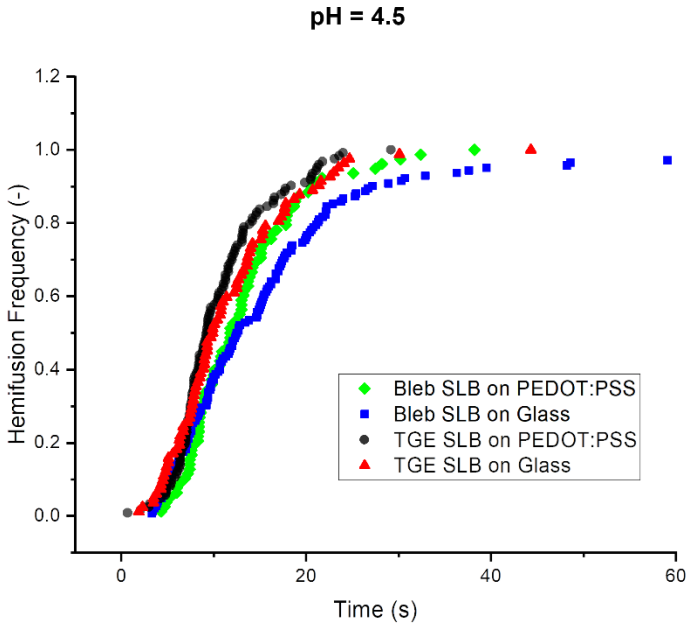

Surface	Bleb	Lipid	k1	N	No. of Particles	Fit
PEDOT	VeroE6	POPC-PEG5K	0.39	4.97	78	0.995
PEDOT	--	TGE	0.53	5.24	123	0.989
Glass	VeroE6	POPC-PEG5K	0.18	2.62	142	0.997
Glass	--	TGE	0.29	3.26	82	0.997

Fig. 17 & Table. 2 **Hemifusion frequency analysis and results.** Cumulative distribution function plot of native influenza X-31 viruses fusing into Vero E6 bleb bilayers and TGE lipid bilayers on different substrates at pH 4.5.

PEDOT:PSS and glass. In addition, more HA proteins were involved in each fusion event on a PD-SLB, as a higher N value of 5 was calculated compared with that for common viral fusion observed on glass, which is around 3. An exact mechanism behind the differences between two substrates is still being investigated, but overall, they produced results that are within the same order of magnitude, which demonstrate that we can observe reasonable viral fusion on PEDOT:PSS for its application as a viral detection method.

2.4. Conclusion

To investigate the compatibility of PD-SLB platforms that we developed in the previous chapter with viral fusion analysis, multiple characterizations were conducted including enzymatic accessibility assay for protein orientation and single virion tracking for influenza X-31 viral fusion. The enzymatic accessibility test demonstrates that membrane proteins that are located on the top leaflet of PD-VeroE6-SLBs were predominately outwards on host cell membranes, indicating a “parachute” rupture mode. This ensures viral receptors (e.g. sialic acids for influenza viruses) that naturally exist on the outer host membranes are available for viruses to bind during a future viral detection, confirmed by substantial specific binding when these bilayers were used. Some deviations were reported for viral fusion kinetics analyzed on PEDOT:PSS substrates and those on glass slides using SPT. This corresponds to our expectations because of the different surface conditions between two substrates, but an exact explanation for this is to be investigated. However, the optical characterizations validate that the virus binding and triggered fusion can proceed as established on

glass-based platforms, which is the fundamental of our viral sensor concept. Furthermore, due to the fact that different enveloped viruses have different properties in their viral genomes (e.g. charges, lengths etc.), we expect them to generate different electrical readouts when released onto an electrochemical device, resulting in a distinct “fingerprint” for each species. Future work includes conducting electrical measurements on influenza X-31 viruses as well as other enveloped viruses to collect an electrical “fingerprint” for each viruses and building a “fingerprint” database as a reference for the future viral detection and identification.

2.6. Acknowledgement

The author would like to thank the National Science Foundation and the Defense Advanced Research Projects Agency for supported the work presented in this chapter. I would like to acknowledge Mark Richards for proposing the enzymatic accessibility assay for protein orientation, and Tiffany Tang for training me on single particle tracking and contributing to the viral fusion experiments.

References

1 Treanor, J. J. *et al.* Efficacy and Safety of the Oral Neuraminidase Inhibitor Oseltamivir in Treating Acute InfluenzaA Randomized Controlled Trial. *JAMA* **283**, 1016-1024, doi:10.1001/jama.283.8.1016 (2000).

2 Liaw, Y. F. *et al.* Effects of extended lamivudine therapy in Asian patients with chronic hepatitis B. Asia Hepatitis Lamivudine Study Group. *Gastroenterology* **119**, 172-180 (2000).

3 Mast, E. E. *et al.* A comprehensive immunization strategy to eliminate transmission of hepatitis B virus infection in the United States: recommendations of the Advisory Committee on Immunization Practices (ACIP) part 1: immunization of infants, children, and adolescents. *MMWR Recomm Rep* **54**, 1-31 (2005).

4 Gerdil, C. The annual production cycle for influenza vaccine. *Vaccine* **21**, 1776-1779 (2003).

5 Prevention, C. f. D. C. a. *Estimated Influenza Illnesses, Medical visits, Hospitalizations, and Deaths in the United States — 2017–2018 influenza season*, <https://www.cdc.gov/flu/about/burden/2017-2018.htm#table1> (2018).

6 Stockton, J., Ellis, J. S., Saville, M., Clewley, J. P. & Zambon, M. C. Multiplex PCR for Typing and Subtyping Influenza and Respiratory Syncytial Viruses. *Journal of Clinical Microbiology* **36**, 2990-2995 (1998).

7 Leland, D. S. & Ginocchio, C. C. Role of cell culture for virus detection in the age of technology. *Clinical microbiology reviews* **20**, 49-78, doi:10.1128/CMR.00002-06 (2007).

8 Hazelton, P. R. & Gelderblom, H. R. Electron microscopy for rapid diagnosis of infectious agents in emergent situations. *Emerging infectious diseases* **9**, 294-303, doi:10.3201/eid0903.020327 (2003).

9 Hedman, K. & Rousseau, S. A. Measurement of avidity of specific IgG for verification of recent primary rubella. *J Med Virol* **27**, 288-292 (1989).

10 Kim, D.-K. & Poudel, B. Tools to detect influenza virus. *Yonsei medical journal* **54**, 560-566, doi:10.3349/ymj.2013.54.3.560 (2013).

11 Garibyan, L. & Avashia, N. Polymerase chain reaction. *The Journal of investigative dermatology* **133**, 1-4, doi:10.1038/jid.2013.1 (2013).

12 Bustin, S. A. & Nolan, T. Pitfalls of quantitative real-time reverse-transcription polymerase chain reaction. *Journal of biomolecular techniques : JBT* **15**, 155-166 (2004).

13 Ali, T. *et al.* Detection of Influenza Antigen with Rapid Antibody-Based Tests after Intranasal Influenza Vaccination (FluMist). *Clinical Infectious Diseases* **38**, 760-762, doi:10.1086/382887 (2004).

14 Faix, D. J., Sherman, S. S. & Waterman, S. H. Rapid-Test Sensitivity for Novel Swine-Origin Influenza A (H1N1) Virus in Humans. *New*

England Journal of Medicine **361**, 728-729, doi:10.1056/NEJMc0904264 (2009).
15 Plemper, R. K. Cell entry of enveloped viruses. *Current opinion in virology* **1**, 92-100, doi:10.1016/j.coviro.2011.06.002 (2011).
16 Hsu, H.-L., Millet, J. K., Costello, D. A., Whittaker, G. R. & Daniel, S. Viral fusion efficacy of specific H3N2 influenza virus reassortant combinations at single-particle level. *Scientific Reports* **6**, 35537, doi:10.1038/srep35537 (2016).
17 Costello, D. A. & Daniel, S. Single particle tracking assay to study coronavirus membrane fusion. *Methods Mol Biol* **1282**, 183-194, doi:10.1007/978-1-4939-2438-7_16 (2015).
18 Floyd, D. L., Ragains, J. R., Skehel, J. J., Harrison, S. C. & van Oijen, A. M. Single-particle kinetics of influenza virus membrane fusion. *Proc Natl Acad Sci U S A* **105**, 15382-15387, doi:10.1073/pnas.0807771105 (2008).
19 Costello, D. A., Hsia, C.-Y., Millet, J. K., Porri, T. & Daniel, S. Membrane Fusion-Competent Virus-Like Proteoliposomes and Proteinaceous Supported Bilayers Made Directly from Cell Plasma Membranes. *Langmuir* **29**, 6409-6419, doi:10.1021/la400861u (2013).
20 Richards, M. J. *et al.* Membrane Protein Mobility and Orientation Preserved in Supported Bilayers Created Directly from Cell Plasma Membrane Blebs. *Langmuir* **32**, 2963-2974, doi:10.1021/acs.langmuir.5b03415 (2016).
21 Floyd, D. L., Ragains, J. R., Skehel, J. J., Harrison, S. C. & van Oijen, A. M. Single-particle kinetics of influenza virus membrane fusion. *Proceedings of the National Academy of Sciences* **105**, 15382-15387, doi:10.1073/pnas.0807771105 (2008).
22 Bernards, D. A. & Malliaras, G. G. Steady-State and Transient Behavior of Organic Electrochemical Transistors. *Advanced Functional Materials* **17**, 3538-3544, doi:10.1002/adfm.200601239 (2007).
23 Owens, R. M. & Malliaras, G. G. Organic Electronics at the Interface with Biology. *MRS Bulletin* **35**, 449-456, doi:10.1557/mrs2010.583 (2010).
24 Matlin, K. S., Reggio, H., Helenius, A. & Simons, K. Infectious entry pathway of influenza virus in a canine kidney cell line. *The Journal of Cell Biology* **91**, 601, doi:10.1083/jcb.91.3.601 (1981).
25 Hsia, C.-Y., Richards, M. J. & Daniel, S. A review of traditional and emerging methods to characterize lipid–protein interactions in biological membranes. *Analytical Methods* **7**, 7076-7094, doi:10.1039/C5AY00599J (2015).
26 Castellana, E. T. & Cremer, P. S. Solid supported lipid bilayers: From biophysical studies to sensor design. *Surface Science Reports* **61**, 429-444, doi:https://doi.org/10.1016/j.surfrep.2006.06.001 (2006).

27 Diaz, A. J., Albertorio, F., Daniel, S. & Cremer, P. S. Double Cushions Preserve Transmembrane Protein Mobility in Supported Bilayer Systems. *Langmuir* **24**, 6820-6826, doi:10.1021/la800018d (2008).
28 Hsia, C.-Y., Chen, L., Singh, R. R., DeLisa, M. P. & Daniel, S. A Molecularly Complete Planar Bacterial Outer Membrane Platform. *Scientific Reports* **6**, 32715, doi:10.1038/srep32715 https://www.nature.com/articles/srep32715#supplementary-information (2016).
29 Tamm, L. K. & McConnell, H. M. Supported phospholipid bilayers. *Biophys J* **47**, 105-113, doi:10.1016/S0006-3495(85)83882-0 (1985).
30 Brian, A. A. & McConnell, H. M. Allogeneic stimulation of cytotoxic T cells by supported planar membranes. *Proceedings of the National Academy of Sciences* **81**, 6159, doi:10.1073/pnas.81.19.6159 (1984).
31 Richards, M. J. *et al.* Membrane Protein Mobility and Orientation Preserved in Supported Bilayers Created Directly from Cell Plasma Membrane Blebs. *Langmuir* **32**, 2963-2974, doi:10.1021/acs.langmuir.5b03415 (2016).
32 Baumgart, T. *et al.* Large-scale fluid/fluid phase separation of proteins and lipids in giant plasma membrane vesicles. *Proceedings of the National Academy of Sciences* **104**, 3165, doi:10.1073/pnas.0611357104 (2007).
33 Brown, J. S. *et al.* Antibacterial isoamphipathic oligomers highlight the importance of multimeric lipid aggregation for antibacterial potency. *Communications Biology* **1**, 220, doi:10.1038/s42003-018-0230-4 (2018).
34 Friedel, B. *et al.* Effects of Layer Thickness and Annealing of PEDOT:PSS Layers in Organic Photodetectors. *Macromolecules* **42**, 6741-6747, doi:10.1021/ma901182u (2009).
35 Rivnay, J., Owens, R. M. & Malliaras, G. G. The Rise of Organic Bioelectronics. *Chemistry of Materials* **26**, 679-685, doi:10.1021/cm4022003 (2014).
36 Horikawa, M. *et al.* The development of a highly conductive PEDOT system by doping with partially crystalline sulfated cellulose and its electric conductivity. *Journal of Materials Chemistry C* **3**, 8881-8887, doi:10.1039/C5TC02074C (2015).
37 Richter, R. P., Bérat, R. & Brisson, A. R. Formation of Solid-Supported Lipid Bilayers: An Integrated View. *Langmuir* **22**, 3497-3505, doi:10.1021/la052687c (2006).
38 Khodagholy, D. *et al.* High transconductance organic electrochemical transistors. *Nature Communications* **4**, 2133, doi:10.1038/ncomms3133 https://www.nature.com/articles/ncomms3133#supplementary-information (2013).
39 Axelrod, D., Koppel, D. E., Schlessinger, J., Elson, E. & Webb, W. W. Mobility measurement by analysis of fluorescence photobleaching recovery kinetics. *Biophys J* **16**, 1055-1069, doi:10.1016/S0006-3495(76)85755-4 (1976).

40 Zhang, Y. *et al.* Supported Lipid Bilayer Assembly on PEDOT:PSS Films and Transistors. *Advanced Functional Materials* **26**, 7304-7313, doi:10.1002/adfm.201602123 (2016).
41 Duc, C., Vlandas, A., Malliaras, G. G. & Senez, V. Wettability of PEDOT:PSS films. *Soft Matter* **12**, 5146-5153, doi:10.1039/C6SM00599C (2016).
42 Seitz, M. *et al.* Formation of Tethered Supported Bilayers by Vesicle Fusion onto Lipopolymer Monolayers Promoted by Osmotic Stress. *Langmuir : the ACS journal of surfaces and colloids* **16**, 6067-6070, doi:10.1021/la9915771 (2000).
43 Boersma, A. J., Zuhorn, I. S. & Poolman, B. A sensor for quantification of macromolecular crowding in living cells. *Nature Methods* **12**, 227, doi:10.1038/nmeth.3257
https://www.nature.com/articles/nmeth.3257#supplementary-information (2015).
44 Berquand, A. *et al.* Two-Step Formation of Streptavidin-Supported Lipid Bilayers by PEG-Triggered Vesicle Fusion. Fluorescence and Atomic Force Microscopy Characterization. *Langmuir* **19**, 1700-1707, doi:10.1021/la0260180 (2003).
45 Richter, R. P. & Brisson, A. R. Following the Formation of Supported Lipid Bilayers on Mica: A Study Combining AFM, QCM-D, and Ellipsometry. *Biophys J* **88**, 3422-3433, doi:https://doi.org/10.1529/biophysj.104.053728 (2005).
46 Dacic, M. *et al.* Influence of Divalent Cations on Deformation and Rupture of Adsorbed Lipid Vesicles. *Langmuir* **32**, 6486-6495, doi:10.1021/acs.langmuir.6b00439 (2016).
47 Lai, A. L., Millet, J. K., Daniel, S., Freed, J. H. & Whittaker, G. R. The SARS-CoV Fusion Peptide Forms an Extended Bipartite Fusion Platform that Perturbs Membrane Order in a Calcium-Dependent Manner. *J Mol Biol* **429**, 3875-3892, doi:10.1016/j.jmb.2017.10.017 (2017).
48 Rogers, G. N. & Paulson, J. C. Receptor determinants of human and animal influenza virus isolates: Differences in receptor specificity of the H3 hemagglutinin based on species of origin. *Virology* **127**, 361-373, doi:https://doi.org/10.1016/0042-6822(83)90150-2 (1983).
49 Soumpasis, D. M. Theoretical analysis of fluorescence photobleaching recovery experiments. *Biophys J* **41**, 95-97, doi:10.1016/S0006-3495(83)84410-5 (1983).
50 White, J. M., Delos, S. E., Brecher, M. & Schornberg, K. Structures and mechanisms of viral membrane fusion proteins: multiple variations on a common theme. *Crit Rev Biochem Mol Biol* **43**, 189-219, doi:10.1080/10409230802058320 (2008).
51 Costello, D. A., Whittaker, G. R. & Daniel, S. Variations in pH Sensitivity, Acid Stability, and Fusogenicity of Three Influenza Virus H3

Subtypes. *Journal of Virology* **89**, 350, doi:10.1128/JVI.01927-14 (2015).
52 Liu, H.-Y. *et al.* Supported Planar Mammalian Membranes as Models of in Vivo Cell Surface Architectures. *ACS Applied Materials & Interfaces* **9**, 35526-35538, doi:10.1021/acsami.7b07500 (2017).
53 White, J. M. & Whittaker, G. R. Fusion of Enveloped Viruses in Endosomes. *Traffic* **17**, 593-614, doi:10.1111/tra.12389 (2016).
54 Zhang, J. *et al.* Cholesterol content in cell membrane maintains surface levels of ErbB2 and confers a therapeutic vulnerability in ErbB2-positive breast cancer. *Cell Commun Signal* **17**, 15-15, doi:10.1186/s12964-019-0328-4 (2019).
55 Yang, S.-T., Kreutzberger, A. J. B., Lee, J., Kiessling, V. & Tamm, L. K. The role of cholesterol in membrane fusion. *Chem Phys Lipids* **199**, 136-143, doi:10.1016/j.chemphyslip.2016.05.003 (2016).
56 Sun, X. & Whittaker, G. R. Role for Influenza Virus Envelope Cholesterol in Virus Entry and Infection. *Journal of Virology* **77**, 12543, doi:10.1128/JVI.77.23.12543-12551.2003 (2003).